SUBDIVISION AND APPROXIMATION OF FREE-FORM STEEL STRUCTURES

Development of a methodology for quadrangular subdivision of free-form steel shapes into optimized producible panels. Implementation in a semi-parametric tool.

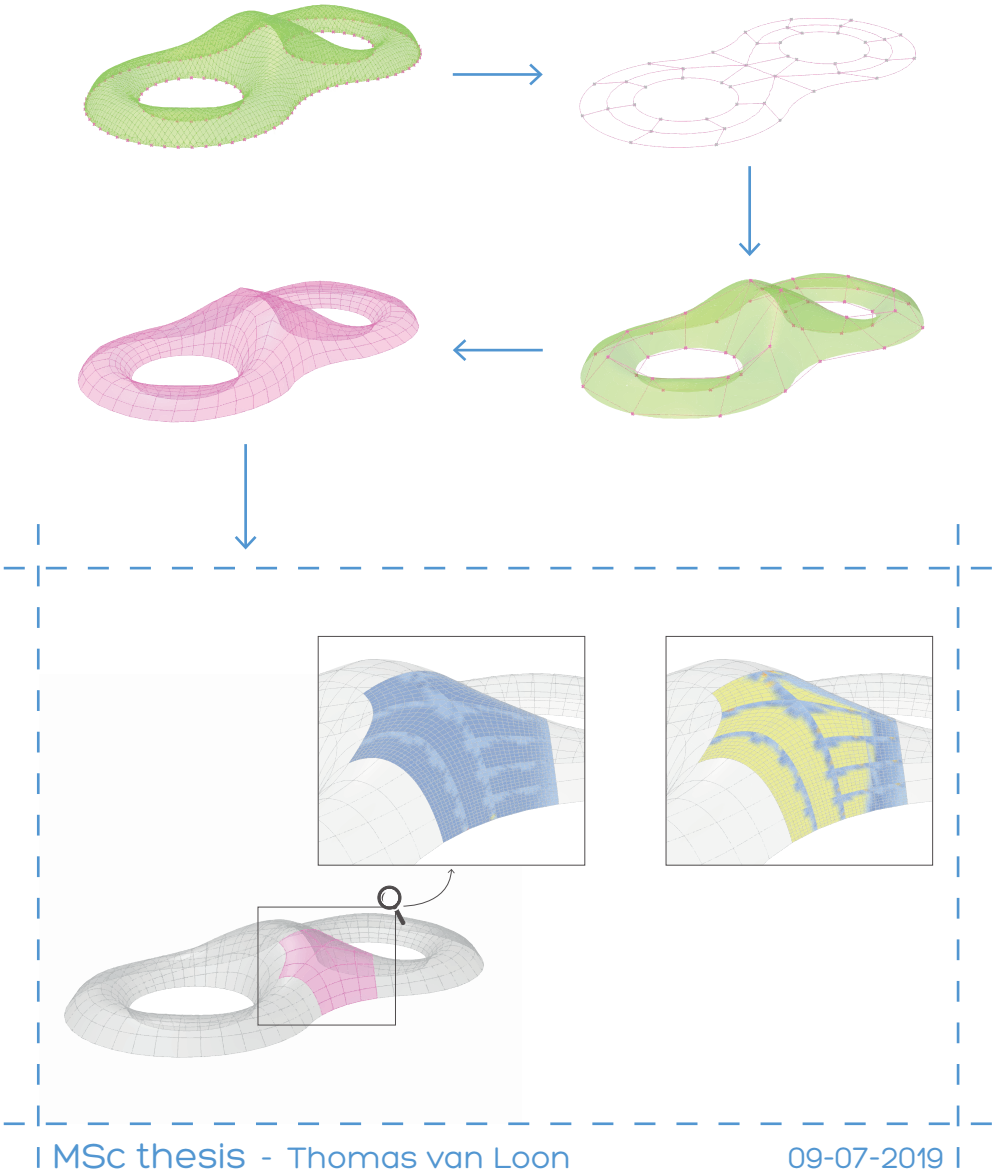

MSc thesis - Thomas van Loon

09-07-2019

Master of Science (MSc) Thesis

MSc Architecture, Urbanism and Building Technology
Master track: Building Technology

Title

Subdivision and approximation of free-form steel structures

Subtitle

Development of a methodology for quadrangular subdivision of free-form steel shapes into optimized producible panels. Implementation in a semi-parametric tool

Date

9th of July 2019

Author

Name: Thomas van Loon
Student nr.: 4350472
Personal e-mail: thomas_vanloon@hotmail.com

Mentor team

1st mentor:	Dr. ir. P. Nourian	AE + T Design Informatics
2nd mentor:	ir. P. Eigenraam	AE + T Structural Design & Mechanics

Delegate of the board of examiners

Dr. D.K. Czischke Ljubetic — Management in the Built Environment

University

Delft University of Technology
Faculty of Architecture and the Built Environment
Julianalaan 134, 2628 BL, Delft, the Netherlands

Table of contents

Planar panels

Złote Tarasy, Warsaw, Poland
Image by Marek Stepan / Alamy Stock Photo[1]

House for Hippopotamus, Zoo Berlin, Germany
Image by Schlaich Bergermann Partner[2]

Developable (single-curved) panels

Fondation Louis Vuitton, Paris, France
Image by TripAdvisor[3]

MGM Park, Shade structures, Las Vegas
Image by [5]

Double curved panels

Hungerburg funicular railway, Innsbruck
Image by Zaha Hadid Architects[4]

1 https://www.alamy.com/stock-photo/zlote-tarasy-warsaw-poland.html

2 https://www.sbp.de/en/project/house-for-hippopotamus-zoo-berlin/

3 https://www.tripadvisor.co.za/LocationPhotoDirectLink-g187147-d7149635-i292928620-Fondation_Louis_Vuitton-Paris_Ile_de_France.html

4 http://www.zaha-hadid.com/2017/12/15/hungerburg-funicular-railway-innsbruck-celebrates-its-10th-anniversary/

5 https://www.alblasserdam.net/nieuws/2016-04-05-9381-nieuw-park-in-las-vegas-toont-werk-royal-ihc.html

1 Introduction

Due to technological innovations free-form shapes in architecture can be seen more often nowadays. For instance in façades, roofs and pavilions. In between this design shape and actual producible shape lays a complex process that has to do with approximating and subdividing this shape in economically producible panels. Restrictions for production depend, of course, on the production techniques that a certain company uses. This could determine if the approximated surfaces will consist out of planar, developable (single-curved) or double curved surfaces. Besides this the fabrication costs of developable panels are much lower than that of double-curved panels. (Ghang & Seonwoo, 2012)

Assembly of the panels is another factor which is of influence. If the design is intended for structural purposes, the edges should have a connection which can transmit the loads through the surface. This could determine what shape the panels (e.g. triangular or quadrilateral) or whether the panel edges should be planar curves or even straight lines. On the other hand, when the design is intended as a façade or interior cladding, the type of connection to the substructure could determine these criteria.

In what kind of material the structure is intended is another interesting factor. Soft materials as paper, carton and even wood can be (slightly) adjusted in shape during assembly to make the pieces fit exactly on the substructure. However, when dealing with a steel structure this is not always the case. Steel panels from a certain thickness need to be produced in the correct shape in the factory and having a completely double-curved surface can make the production time, and therefore also costs, rather high. Especially for architectural purposes in comparison to for example the car industry, because (most) panels are unique. Besides, during the forming of double-curved panels the material will be stretched and deformed along the edges, which may lead to connection problems later on.

Therefore planar or developable (single-curved) panels are better in respect to the production. The challenge here is to approximate any arbitrary shape with these type of panels. Since the aesthetics of a surface, which can be described as smoothness, is highly important in architectural applications, the developable panels may provide a more suitable solution and reach a higher accuracy with the approximation of the original shape.

2 Background

The (double-)curving of steel panels has been done for years in the shipbuilding industry. One company in this field is Royal IHC. They are able to produce double-curved steel panels in many shapes, sizes and thicknesses. AIP Partners, an architectural spin-off company of Royal IHC, uses the machinery available at the Royal IHC production halls for architectural purposes. Applications range from interior finishing to exterior finishing and even self-supporting structures such as pavilions. The latter is possible due to the excellent structural properties of the steel. However, according to Mick de Haan (working at AIP Partners) the steel load bearing structures have been realized by just increasing the sheet thickness up to even 25mm. With the machinery available at the Royal IHC production halls the forming of single- or double curved steel sheets – even up to this thickness – is possible, but rely deeply on the manual work of skilled workers. The only full CNC-controlled machine available is the plasma-cutter. (M. de Haan, personal communication, 24 October 2018)

Concerning the forming of (double-)curved steel panels new innovations exist, for example flexible multipoint forming, flexible stretch forming and innovative adjustments to incremental sheet forming processes. However, these still have their own problems that reduce the accuracy and smoothness of the final product such as possible dents in the surface, wrinkling, tearing, local thinning of the surface and springback in the material. An overview of the advantages and restrictions of several existing production processes is included in the literature study in the Appendix. Besides the disadvantages mentioned before, forming thick sheets as the ones used by AIP Partners for self-supporting structures, is not possible with these production methods.

Visit Royal IHC production halls[1]

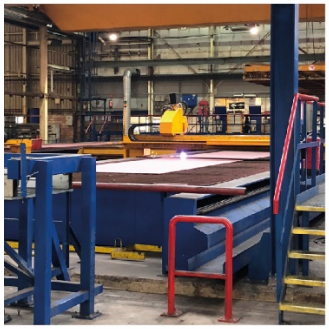

Plasma cutter

'Kantbank' using Press Forming

Press, also using Press Forming

'English wheel' using Roll Forming

MDF 'ribs' for checking curvature

1 Pictures shown are own images

3 Problem statement

As described above, the production process of AIP Partners relies very on the manual handling of the work pieces which consumes a lot of time – and therefore costs – and makes it difficult to guarantee the desired accuracy of the final product. Especially for double-curved panels, where the production time could rise 10-12 times higher compared to single curved panels. (M. de Haan, personal communication, 24 October 2018) Current optimizations take place to reduce the number of double-curved panels and replace them by single curved panels with the best approximation to the original surface. However, this is still a manual process and handles one panel at a time.

New innovative production methods for the forming of (double-)curved steel sheets still present flaws, most of them specifically related to double-curved panels due to unequally distributed strain in the workpiece. Besides this, most existing companies have a complete working production line with certain production methods, and do not have the capacity or are not willing to invest in new expensive production methods. In this case a new innovative use of their existing machinery would be more interesting.

The way AIP Partners realizes self-supporting structures is mostly related to their traditional production process, but increasing the stiffness of the panels by increasing only the thickness, requires a large amount of extra material and therefore increases the embodied energy of the final structure significantly.

4 Objective and scope

4.1 Objective

The above described problems led to a desire to develop a method for manufacturing free-form structures – with a guarantee for high accuracy – using the available production processes for AIP Partners. This consists partly of an approximation of the original surface and developing a method for increasing the structural properties of a panel if a self-supporting structure is desired.

Computational design tools could shorten the product development cycle if aspects such as fabrication, material properties and structure (connections) are integrated into the design process. (Pottmann et. al, 2014) Therefore the objective is to develop a semi-parametric tool which subdivides free-form steel shapes in optimized producible panels. Optimized in this context means that the panels should approximate the designed shape with the highest accuracy and smoothness possible. Semi-parametric means there could still be manual inputs based on design requirements. Since the designing takes place in a parametric environment, this opens up possibilities to include an structural validation for self-supporting structures, based on a FEM-analysis, within the tool.

Since the end product is used for architectural applications the aesthetics are an important factor. These inputs could for instance be maximum panel dimensions and panel shapes. The focus however will be on the use of developable surfaces, since these can make smoother shapes than polyhedral surfaces.

4.2 Scope

As briefly discussed in the problem statement and objective, the scope of this research lays on the one hand on automatically generating quadrangular grids on a surface, and on the other hand a geometrical approximation of the original surface, based on the requirements related to the production and material. For this research the approximation has a main focus on developable (i.e. single-curved) panels. On the other hand a method for creating self-supporting structures using less material – and therefore reducing the embodied energy – will be developed.

5 Research questions

The main research question based on the objective of this research can be formulated as the following:

> *"How can free-form steel shapes be approximated by individual panels in order to prepare for the production?"*

The answer of this main question can be found in several different fields of research. The question is therefore split into several sub-questions related to different parts of the question These sub-questions are formulated as the following:

- *What are the restrictions and limitations of the production and how do they affect the panel shapes and sizes?*
- *How can a grid be automatically generated on an arbitrary shape?*
- *How can a double curved panel be rebuild into a developable surface and how to implement this for a shape formed by multiple panels?*
- *What influence does the subdivision have on the developable surfaces and how does this affect the accuracy?*

In order to answer the previously mentioned questions, a literature study is done. Research is done in three different main areas. The first being the approximation of (free-form) surfaces. Keywords for this were *shape approximation, double-curved, single-curved, developable surfaces*. From the literature more useful keywords as *architectural panelization, developable stripes and curved folding* were found. Since curved folding is based on developable surfaces some useful definitions for developability were found.

Secondly research is done on methods to initialize a quad mesh on an arbitrary surface, Keywords for this were among others *generating grids, quadrangular subdivision, quad meshes, quad grids*. Most useful literature was found on the topic of creating a quadrangular grid based on the topology of the surface, therefore other used keywords were *Medial Axis* and *topological skeleton*.

Parallel to these studies, research is done in production methods for curved steel panels. Keywords for this were *manufacturing of sheet metal, sheet bending, producing (double-)curved sheet metal*. More useful literature was found in the field of bending metal sheets, rather than steel in particular. However, authors claim most of the described methods were also applicable for thin steel sheets. The results from this study formed the basis for the approach followed in this research

Based on the results from the literature study an approach and methodology is developed that will be implemented in several Grasshopper definitions in order to validate and execute the method parametrically. The complete literature study can be found in the Appendix.

6 Approach

As discussed earlier, there is aimed to develop a method to make the double curving of sheets possible with existing machinery and a guaranteed high accuracy. Next to this, the method should include the possibility to create self-supporting structures without using thick steel plates with a high embodied energy. The innovations in the field of forming curved sheet metal discussed earlier lead to complex processes that demand new machinery and tools, what makes it hard for most companies in this field to change their production line. For this reason the focus will be on creating an innovative solution with the available production methods.

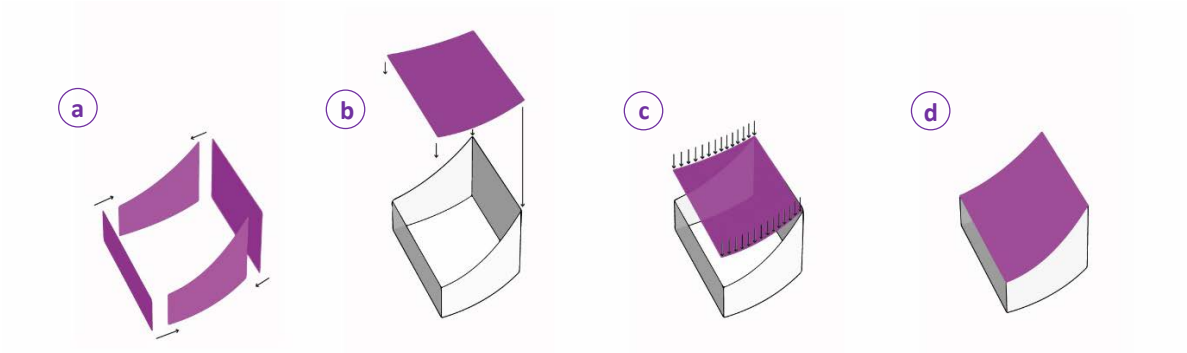

Figure 1: Principle of proposed production method.

Since the only full CNC-controlled machine available is a plasma-cutter, there is aimed for a method with sandwich constructions based on the research of Bailly et al. (2015), but with a different design. For this research a method is suggested where the plasma cutter is used to create ribs for the sandwich panels, these can be cut very accurate. These ribs will be assembled according to their corresponding angles (Figure 1a), possibly with reinforcement in the corners if necessary. All the single-curved sheets are unrolled into 2D sheets for the laser cutting, followed by placing them on the frame (Figure 1b). The unrolled sheets are forced into the correct shape using the frame as a guide. (Figure 1c and Figure 1d) However, additional research must be done to what extend this is possible for thin steel sheets, in particular up to which thicknesses. Hybrid forming methods with the available production methods could provide a solution as well. Sheets could be pre-curved using press forming, and then placed on top of the guiding frame to make up for the springback and other inaccuracies during the forming process.

In this way the assembled structure could be seen as a grid-shell, where the curved sheets would serve as finishing and could provide the necessary shear stiffness. The reach of the lateral stability should be checked and possibly local stiffeners must be added to prevent the curved sheet from buckling. For the assembly of the panels a simple connection with rivets or nuts and bolts is proposed in order to keep the structure demountable. Figure 2 shows a visualization of the assembly with nuts and bolts, it should be noted that for these connection methods either the top- or bottom sheet must have small openings for tightening a bolt during the assembly. However, further research could provide other connection methods for the assembly.

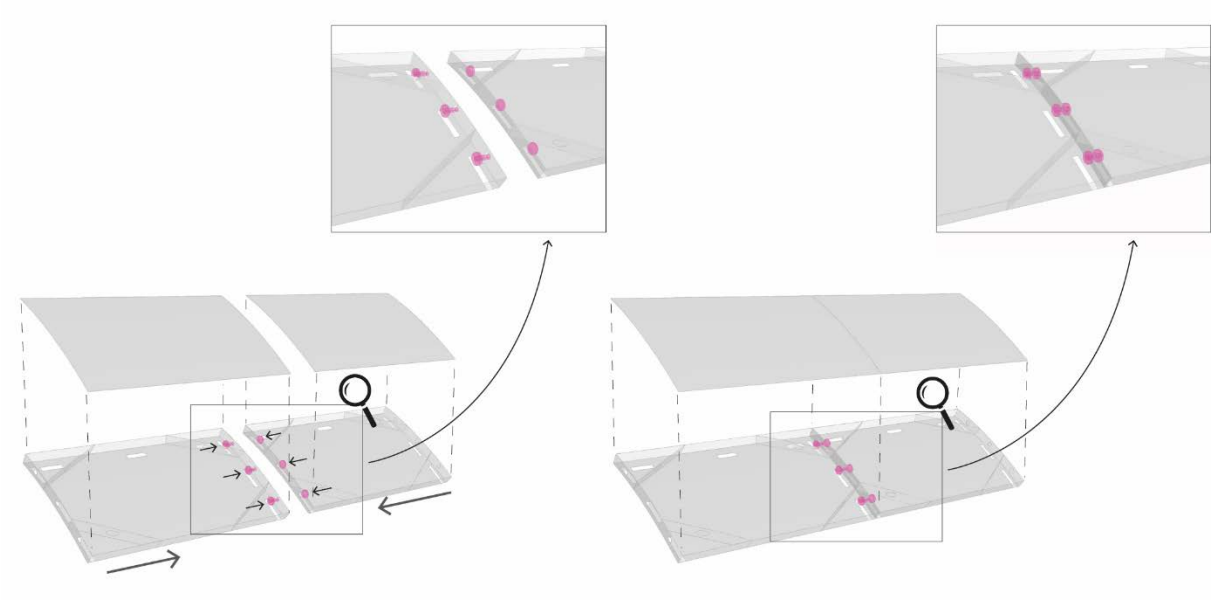

Figure 2: Visualization of assembly proposal with rivets or nuts and bolts. It should be noted that either the top- or the bottom sheet should include openings in order to assemble the panels.

In order to set up a framework which prepares arbitrary shapes for the proposed production approach, independent of the exact assembly method, the objective can be subdivided into 3 main parts:

1. Quadrangular subdivision of the shape. This part will focus on automatic generation of quadrangular grids based on the topology of the shape. The resulting quad mesh will form the input of the second part of the framework.
2. Surface approximation. This part will focus on rebuilding the panel surfaces by increasing the developability of each panel. This challenge will be approached as a global optimization problem, since the panel alignment and smoothness of the global shape are a main priority. The resulting panel surfaces will form the input for the third and last part of the framework.
3. Generating the structural system and performing a preliminary structural analysis. This part will first focus on creating the sandwich structure of each panel, followed by a preliminary structural analysis which provides global dimensions of the structure.

7 Methodology

As mentioned before, the method pursued in this research consists out of three main parts. The first part deals with the quadrangular subdivision of the shape, which can be seen as the process of panelization. (Pottmann et al., 2014) For the second part, the panels based on this panelization are rebuild in order to approximate the original shape as accurate as possible, while increasing the developability for each panel (i.e. using single-curved panels). This process of rebuilding the surfaces can be seen as the process of rationalization. (Pottmann et al., 2014) The third and last part converts the final panel surfaces to the structural sandwich panels and validates the structural performance of the whole shape.

7.1 Subdivision of the shape

The subdivision of the surface can be seen as the process of panelization. (Pottmann et al., 2014) For the purpose of this research a quad division will be used. However, for shapes with a complex topology, such as Breps existing out of multiple surfaces, standard (u,v)-parameterizations might not be suitable of even possible. In order to initialize a quad grid on a shape independent of the surface topology, a method based on the research of Tam and Armstrong (1991), Rigby (2003) and Oval et al. (2018), is implemented in a Grasshopper definition. In Section 6.2.1 this research is explained.

It should be noted that this method works for planar surfaces, not 3-dimensional surfaces. This has to do with the fact that the mesh is based on the Medial Axis of the object surface, which is retrieved from a Delaunay triangulation and the circumcentres of each triangle. In a 3-dimensional shape these circumcentres are located outside the shape, which makes it impossible to construct a proper topological skeleton as base for a coarse mesh. The approach followed in for this method, projects the shape onto the XY-plane and uses these projected boundary curves to construct a coarse mesh. In this way this method can be applied to three dimensional shapes with complex topologies, with exception for the shapes that cannot be projected on the XY-plane – or any other plane – without intersecting themselves.

This chapter is subdivided into 4 paragraphs. In the first paragraph the success of the approach is proved by applying it to a relatively simple shape with only one opening in the shape. In the second paragraph the method will be applied to a more complex shape, which has multiple openings and higher curvatures in the boundary curves as well as the shape itself. In this example the limitations of the method will become clearly visible due to the extreme geometry. These limitations are discussed in the third paragraph, followed by a brief discussion about grid optimizations related to principal curvatures in the shape.

7.1.1 Proving the method

The Grasshopper definition is designed for a shape with the same topology of the shape used in the research of Oval et al. (2018). When this definition was proved to work, it was later implemented to a more complex shape, which will be discussed in the next paragraph. For the construction of the coarse mesh the same steps were followed as described in Section 6.2.1, of which the steps (a-f) are visualized in Figure 3.

a. The first step is projecting the boundary curves onto the XY-plane and dividing these projected boundary curves in a collection of points densely distributed along the boundaries. It should

be noted that the boundary curves of the shape form the input for initializing a coarse quadrangular mesh topology, the exact shape of the mesh is not important at this stage.

b. This step is followed by triangulating the division points using a Delaunay triangulation. This Delaunay triangulation also constructed mesh faces within the opening, but faces of which the centroid is located outside the projected surface boundaries are culled. This leaves a Delaunay mesh between all boundary curves, in which we can identify 3 different faces based on their number of adjacent faces. Singular faces, which are the faces that are adjacent to 3 other faces, form the key element in this method. Their circumcentres are defined as singular points S. Furthermore are the faces with an adjacency of 2 defined as regular faces, and the faces with an adjacency of 1 as corner faces. The latter type has a vertex located on a convex corner of the shape, these points are defined as corner points C.
c. The next step is retrieving the circumcentres of each face to construct the medial axis by interpolating the S-S branches and S-C branches through all the circumcentres of adjacent faces. This provides us with the Medial Axis of the projected shape.
d. In order come to a workable quadrangular topology the Medial Axis is modified by culling the S-C branches. This results in a curve which flows in the main parametrization direction of the shape.
e. The last step is constructing the S-B branches. The B-vertices are the corner vertices of the singular faces. This step introduces the singular points in the topology, located at the circumcentres of the singular faces S, which are points where more than 4 edges meet.
f. The output of the previous step, together with the boundary curves, forms a coarse quadrangular topology which is used as input for the meshing. The end points of the curves represent the vertices of the mesh, and the curves itself represent the connections between the vertices.

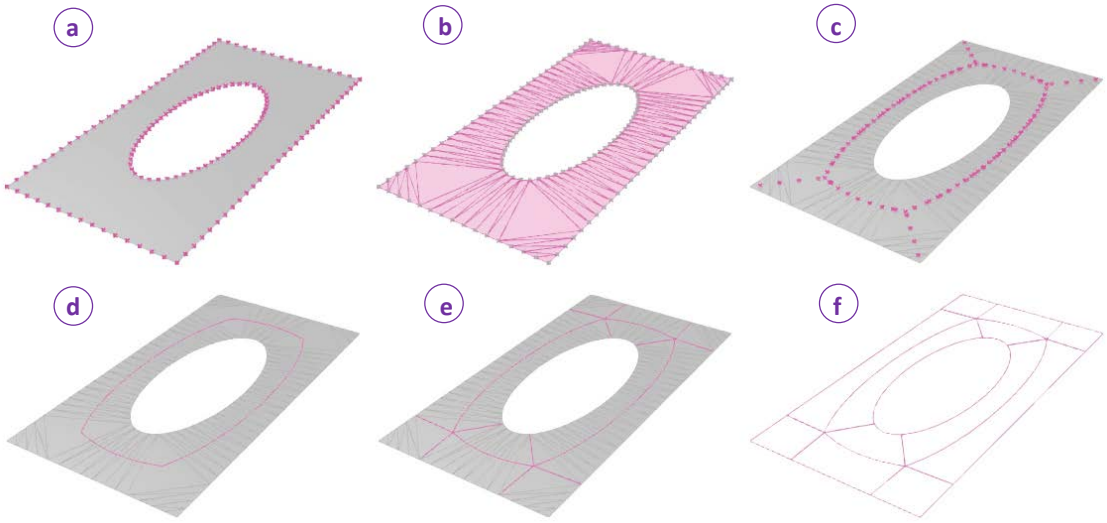

Figure 3: Implementing the method of Oval et al. (2018) into a Grasshopper definition to contruct the topological skeleton.

The created topology is the basis of the coarse quadrangular mesh, but the curved lines cannot be directly converted to mesh edges directly, so each curve is split at the intersection points. In this way the start and end points of all the curves form the vertices of the coarse quad mesh, and the curves represent the connections. It should be noted that this conversion will interpolate straight edges

between the vertices and the mesh will therefore deviate from the initial curved shape of the inner boundary curve. However, the exact geometry of the mesh will be approximated after the topology and density of the mesh are defined. Now the coarse quadrangular mesh is set, it can be subdivided to the desired density using subdividing methods such as the Catmull-Clark subdivision. (Figure 4)

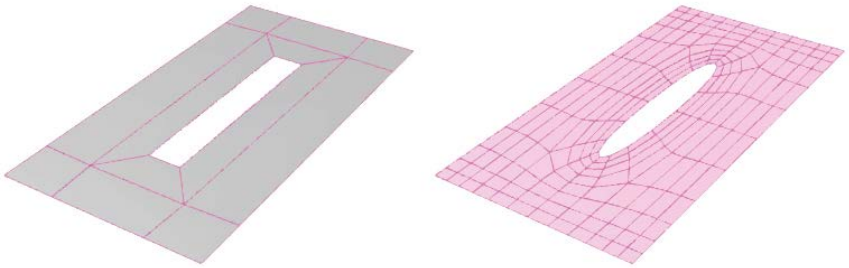

Figure 4: The constructed quad mesh based on the connectivity of the topological skeleton (left), and a densification and smoothening of the mesh using a Catmull-Clark subdivision. (right)

Now the mesh topology is initialized, it can be mapped back onto the 3-dimensional design surface, in this case this is simply done using a projection along the Z-axis. (Figure 5) If desired there could be an extra step which relaxes the mesh on the shape based on additional goalobjects to result in a more equally distributed edge length, this will however be discussed in the next paragraph, since this step is mandatory when dealing with with more complex shapes. The output grid represents the panelization of the object and will be used as input for the rationalization part.

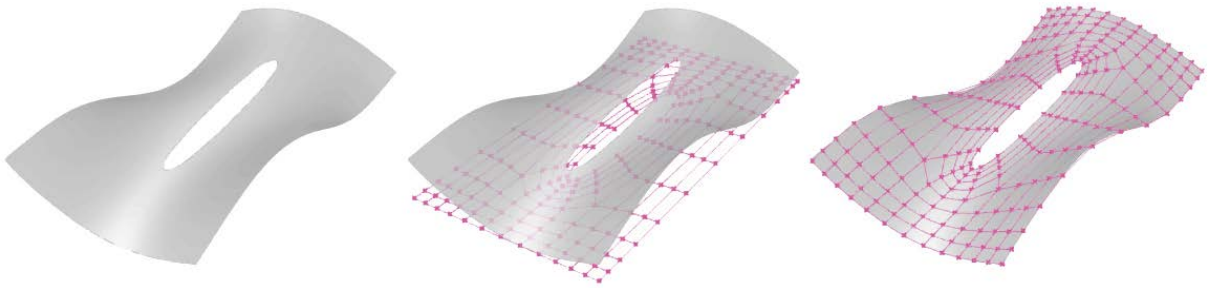

Figure 5: Mapping the constructed mesh onto the 3-dimensional design surface.

Although the final geometry used for the production needs to be modelled as NURBS, meshes will be used for the rationalization since they include information such as connectivity, which is essential for the modifications made in the geometry.

7.1.2 Applying the method to a complex shape [type of input: Brep]

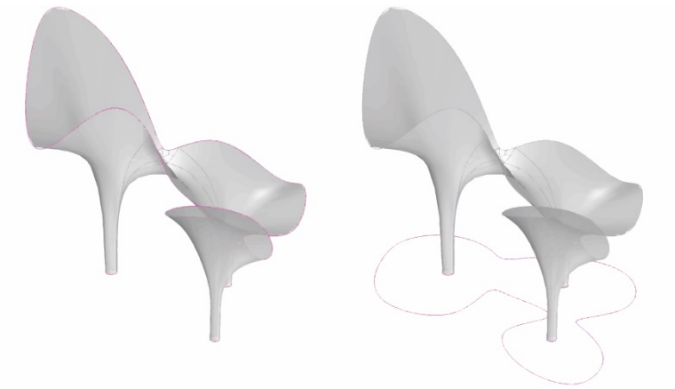

Figure 6: Shape with complex topology for quadrilateral subdivision (left), boundary curves projected on XY-plane as base for the definition (right).

In the previous paragraph the definition is proved to be working, given a test surface with a relatively simple topology. For the purpose of this research a more complex shape is used, this shape is shown in Figure 6. The shape represents a Pavilion named Chengdu Flowers, designed by Melk! Architects. The design was intended to build with steel sheet elements, unfortunately the pavilion was never built. This 3-dimensional double-curved shape has three openings in the shape, located at the supports. Besides the multiple openings, the boundary curves have relatively high convex- and concave curvatures. The extreme geometries in this shape are pushing the algorithm to its limits which is necessary in order to identify what type of limitations might occur.

As input for the definition, the projected boundary curves on the XY-plane are used. Figure 7 shows the different steps necessary to construct the topological skeleton. The steps are similar to the ones described in the previous paragraph, but the definition behind it is more complex and includes some additional steps necessary because of the more complex shape.

The Grasshopper definition designed in the previous paragraph is applied, but several changes were necessary in order to come to the desired result for this complex shape. The method for initializing a coarse quadrangular topology for this complex shape will be categorised in steps (*a* – *j*) for explanation purposes. The steps are visualized in Figure 7.

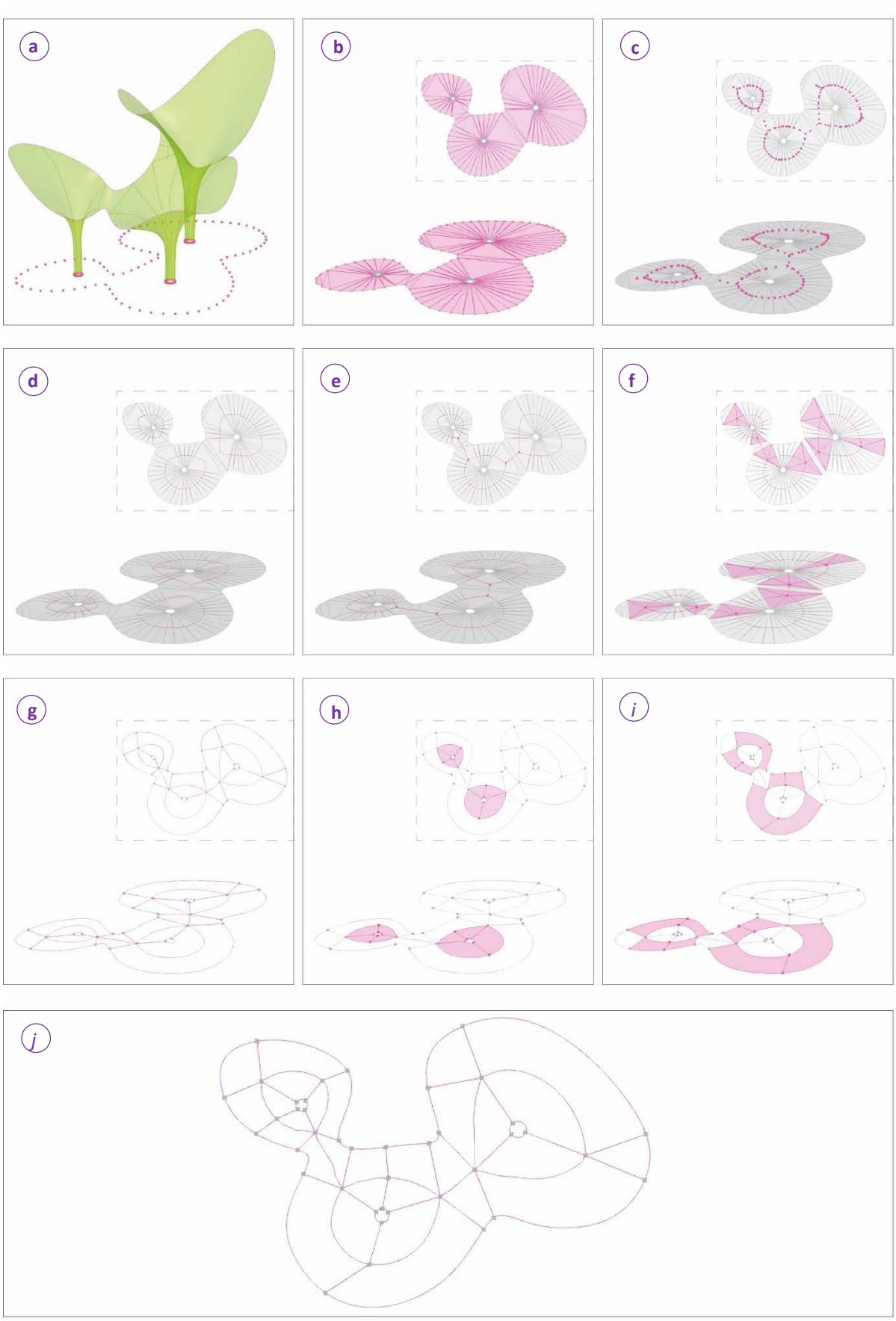

Figure 7: Different steps in constructing the topological diagram of this complex shape.

a. The first steps are similar as the steps described in the previous paragraph. The boundary curves are projected onto the XY-plane and these projected boundary curves are divided into a collection of points densely distributed along the boundaries. The topology will be initialized based on these boundary curves and this point cloud, afterwards this will be mapped onto the object for the actual meshing.
b. This step is followed by triangulating the division points using a Delaunay triangulation. This triangulation created faces within the opening curves, just as with the shape in the previous paragraph. However, in the concave curvatures of the closed boundary curve are also faces created. For these faces another step in the algorithm is necessary which culls these faces. This leaves a Delaunay mesh between all boundary curves, in which we can again identify 3 different faces based on their number of adjacent faces.

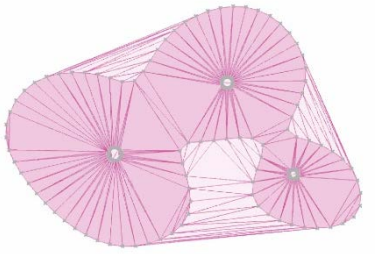

Figure 8: Original Delaunay triangulation, including the faces created outside the domain of the shape.

    1. Singular faces, which are the faces that are adjacent to three other faces. Their circumcentres are defined as singular points S.
    2. Normal faces, which are the faces that are adjacent to two other faces.
    3. Corner faces, which are the faces that are adjacent to only one other face. Therefore they have two of the three edges located on a convex corner of the shape, the vertex connecting these two edges is defined as corner point C.

c. The circumcentres of each face are retrieved in order to construct the Medial Axis. For the shape used in the previous paragraph this was done by interpolating the S-S branches and S-C branches through all the circumcentres of the adjacent faces. However, with this complex shape – which has multiple openings – this method cannot be applied directly and is split in steps *d* and *e*.
d. The Medial Axis in the example from the last paragraph consisted out of a closed polyline around the opening (S-S branches) and four open polylines (S-C branches). This shape however, needs two extra open polylines connecting the S-vertices and forming a connection between the closed polylines around the openings. In this step, the closed polylines around the openings are constructed forming the first part of the S-S branches.
e. In this step, the S-S branches connecting the closed polylines from the previous step are created. Since the required parts of the Medial Axis are constructed manually, there is no need to cull the S-C branches now since these are not created in the first place.
f. For this step, *step e* from the previous paragraph is executed again, which constructs the S-B branches. The B-vertices are the corner vertices of the singular faces, which means that the circumcentres of the singular faces (S) are connected to each corner vertex of this face. This creates singular vertices in the structure, which are vertices where more than 4 edges meet. These singular points form the key in this method, they provide the necessary change in the parameterization directions of the quads in the topology.

g. The output of the previous step, together with the boundary curves, forms a coarse quadrangular topology. The end points of the curves represent the vertices of the mesh, and the curves itself represent the connections between the vertices. In the contrary with the shape in the previous paragraph, this topological diagram cannot be used for meshing directly. The regions adjacent to two of the three openings share all 4 vertices (these are the highlighted regions in Figure 7h) which means that after the meshing, non-manifold faces arise. These regions therefore need to be split into two, so that no region shares all of its vertices with another region. In order to do this two additional steps *h* and *j* are implemented in the definition.

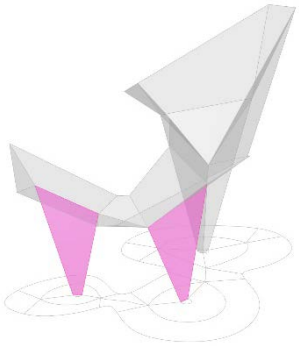

Figure 9: Non-manifold mesh based on the topological diagram created in step a-f. Non-manifold faces are highlighted.

h. This part of the algorithm selects the opening curves which have only two regions adjacent to it. Secondly it selects the regions which have at least one of their edges on that opening curve. selects this curve and also finds the opposite curve. These two curves are then divided at their midpoint, followed by the interpolation of a line through these created points. This line represents a new edge which subdivides the original regions into two regions.

i. The algorithm described in *step h* is repeated for another iteration, since the result of the previous step created new vertices halfway an edge of the adjacent region. A mesh cannot have a vertex halfway an edge, and therefore these regions will not be connected to each other if a mesh would be initialized based on this topology. Only for this iteration the input will not be the opening curves of the shape, but the opposite edges which have been selected in the previous step.

j. The output of *step i* provides the final topological diagram which represents the connectivity of a coarse mesh. The points in the diagram represent the vertices of the mesh and the curves connecting them represent the connections.

In the constructed topological diagram several 3-sided regions exist, which will be translated to triangular mesh faces during the meshing. Since the goal of this approach is to reach a quadrangular subdivision, triangular faces should be avoided. The most simple way to convert a 3-sided region to a 4-sided region is to split one of the edges at its midpoint. (Figure 10a) This approach will lead to a blunt angle in the quads. However, the geometry is not important at this stage, only the topological connections matter. Another approach is described by Tam and Armstrong (1991), as discussed in Section 6.2.1, divides the whole region in three smaller regions as shown in Figure 10b.

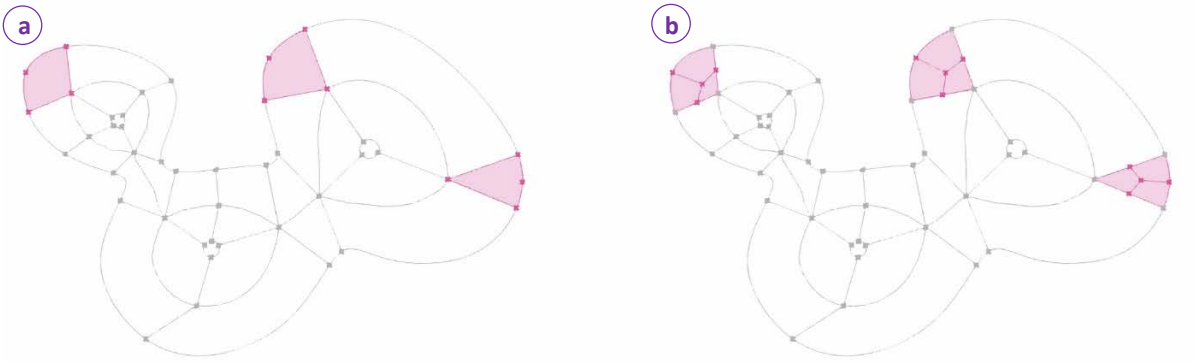

Figure 10: Modifying 3-sided (i.e. triangular) regions to 4-sided (i.e. quadrangular) regions by (a) splitting one of the edge curves at its midpoint or (b) subdividing these regions following the approach described by Tam & Armstrong (1991)

It should be noted that the topological diagram from the second method cannot be used directly as input for the mesh initialization. This has the same reason as discussed in *step h* of the definition, namely the existence of vertices located in the halfway an edge. However, for the subdivision of the coarse quad mesh to the desired density a Catmull-Clark subdivision is used, which subdivides triangles similarly as the method described by Tam & Armstrong (1991) shown in Figure 10b. These two methods of dealing with these triangular faces in the meshing lead to different solutions as shown in Figure 11. How these results are achieved will be explained from the next alinea on. For each method the accuracy of the approximation after rebuilding the panel surfaces needs to be compared in order to choose the best solution. These different approaches for handling triangular faces in convex corners lead to different parameterization directions and therefore might influence the approximation results.

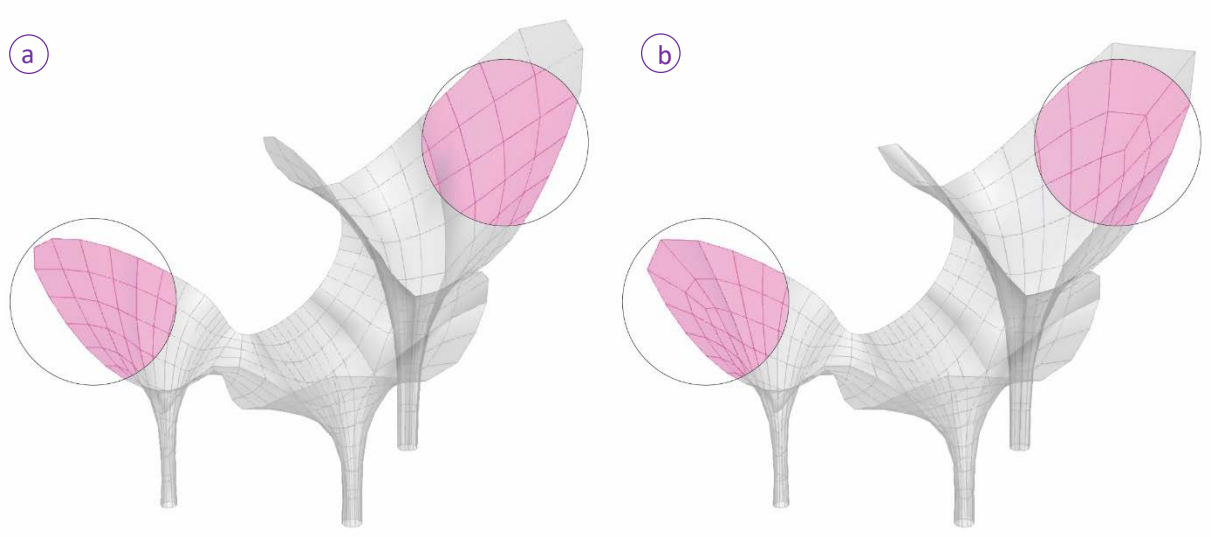

Figure 11: Result in the final mesh using the different treatments for 3-sided regions discussed before. (a) The result of the method from Figure 10a and (b) the result of Figure 10b.

However, during the development of the algorithm itself is continued with the topological diagram from Figure 7j, since the Catmull-Clark subdivision converts all faces to quadrangular faces. The next steps are to convert this topological diagram to a quadrangular mesh and relax it onto the shape. The method for this is subdivided in steps (*a – f*) and visualized in Figure 12.

a. The first step is to project the points back on the surface, before initializing a coarse mesh based on the connectivity of the topological diagram. This is different than the method pursued for the shape in the previous paragraph, where the complete mesh – including the subdivision – was constructed in the XY-plane. The reason for this is that with more complex shapes, especially with high convex- and concave curvatures, faces may intersect partly in the 2D domain. So the points of the topological diagram are projected along the Z-axis back onto the 3D shape, and lines are created between the points based on the connectivity of the topological diagram.
b. This 3 dimensional line structure is then converted to a coarse mesh, where each face consists out of 4 vertices that all lie on the object Brep. However, the mesh deviates significantly from the desired shape, due to the low resolution.
c. In this step the coarse mesh that was constructed previously is subdivided to the desired density of the panels by applying the Catmull-Clark subdivision method. As mentioned previously, this method automatically converts the triangular mesh faces to quadrangular faces in a similar way as described by Tam & Armstrong (1991) shown in Figure 10b.

d. The newly created vertices are not located on the Brep of the object, therefore another iteration of projecting the vertices onto the Brep is necessary. This is done by finding the closest point of each vertex on the Brep and pulling the vertices to that point using the Kangaroo2 plug-in for Grasshopper.
e. By now all the vertices of the mesh lie on the Brep and the desired density of the panels is set, the final step is to relax this mesh onto the Brep using a dynamic relaxation. For the dynamic relaxation the Kangaroo2 plug-in for Grasshopper is used again. For the relaxation several objectives were set with corresponding strengths in order to come to a desired solution. Each objective is assigned a strength, which is a relative value. These values can be adjusted in order to compile a desired panelization. The objectives and their relative strengths used for this relaxation are:
    1. *Points on Mesh (OnMesh)*: The Kangaroo2 library does not include any components to keep points on a Brep, therefore a high resolution mesh is constructed for the Brep. With a high resolution this mesh will resemble the original Brep of the Object. This objective ensures all mesh vertices stay on the object shape.
       Strength: 100
    2. *Points on Curve (OnCurve)*: For the naked vertices, which are the vertices located at the boundaries of the mesh, another objective is set. This objective pulls all these naked vertices to the corresponding boundary curve to ensure the mesh is covering the entire shape.
       Strength: 5000
    3. *Edges as springs (Length (line))*: This component is used twice, first on the naked edges of the mesh. These are the edges located at the boundaries of the mesh. The objective for these edges is to reach an average value, which forces the naked vertices to be evenly spread along the boundary curves.
       Strength: 25
    4. *Edges as springs (Length (line))*: This objective refers to the clothed edges in the mesh, which are all other edges than the naked edges. The objective for these edges is to reach zero length, which provides a smoothening effect for the edges along the object shape.
       Strength: 10
f. The result of the quadrangular panelization after dynamic relaxation of the mesh. This mesh could be used in the Shape Approximation described in Section 7.2.

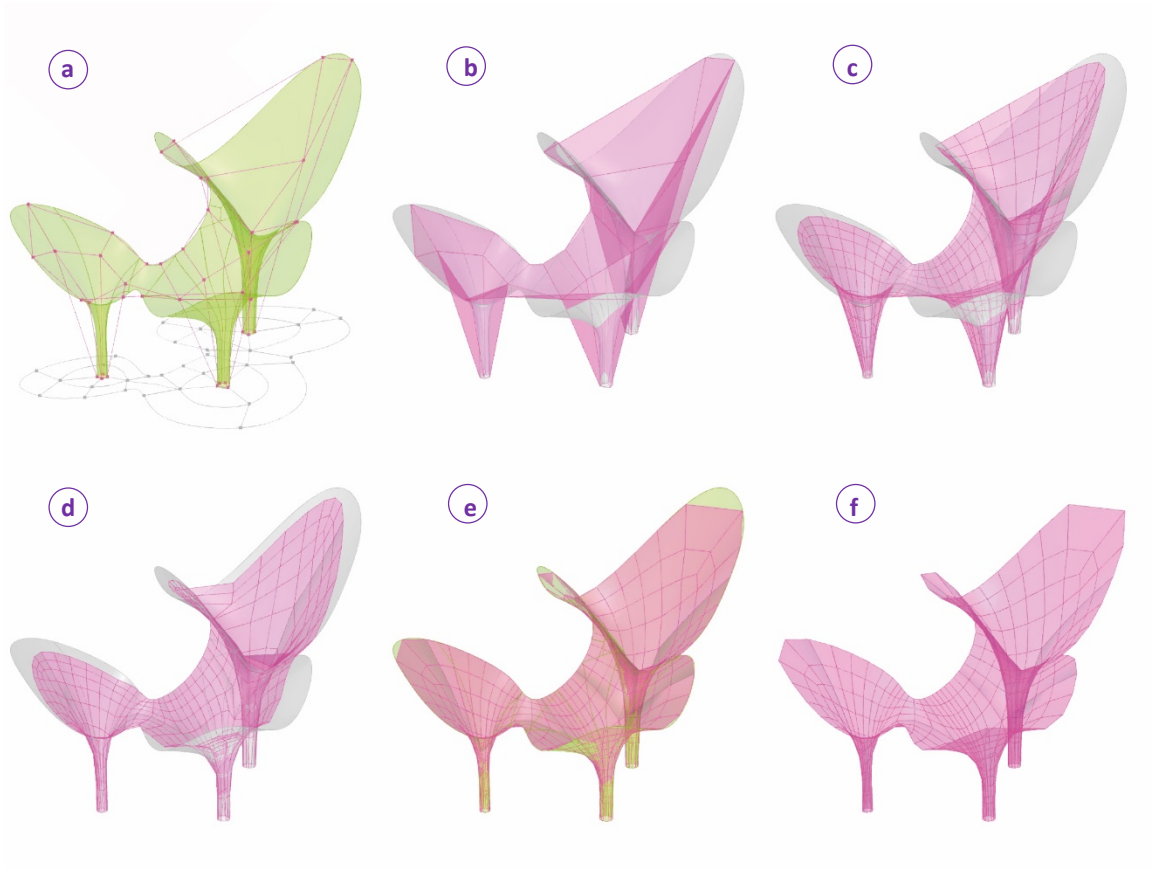

Figure 12: Different stages of mapping the coarse mesh onto the 3-dimensional design shape, subdividing the mesh and relaxing the mesh onto the shape.

7.1.3 Limitations of the method

As mentioned in the introduction of this section, using a complex shape with multiple openings and high curvatures in the boundary curves, as well as the shape itself, pushes the method to its limits. The limitations of this method therefore become quite visible. The first thing that can be seen is that high convex- and concave curvatures lead to rugged boundaries in the final mesh. The magnitude of this problem can be reduced by increasing the density of the mesh or the prevention of high curvatures in the boundary curves. Another limitation is caused by the fact that this specific shape starts from three very narrow circles and diverges considerably towards the top of the shape. Since the subdivision is applied equally on every mesh face in the coarse mesh, panels towards the narrow supports of the structure might become undesirable narrow, while panels towards the top of the shape might become undesirable large.

7.1.4 Applying the method to a mesh [type of input: mesh]

In many design processes (double-)curved shapes arise via form finding methods, for example with Kangaroo. This plug-in is previously used for relaxing the generated quad mesh on the original Brep. However, shapes created with form-finding using Kangaroo are already meshes. In this paragraph the method is applied to a mesh as input geometry. Figure 13 visualizes the steps for creating the topological diagram for this mesh. Since the topological diagram is completely based on the boundary curves of the shape, no changes need to be made in the definition, except for extracting the boundary curves from the input mesh.

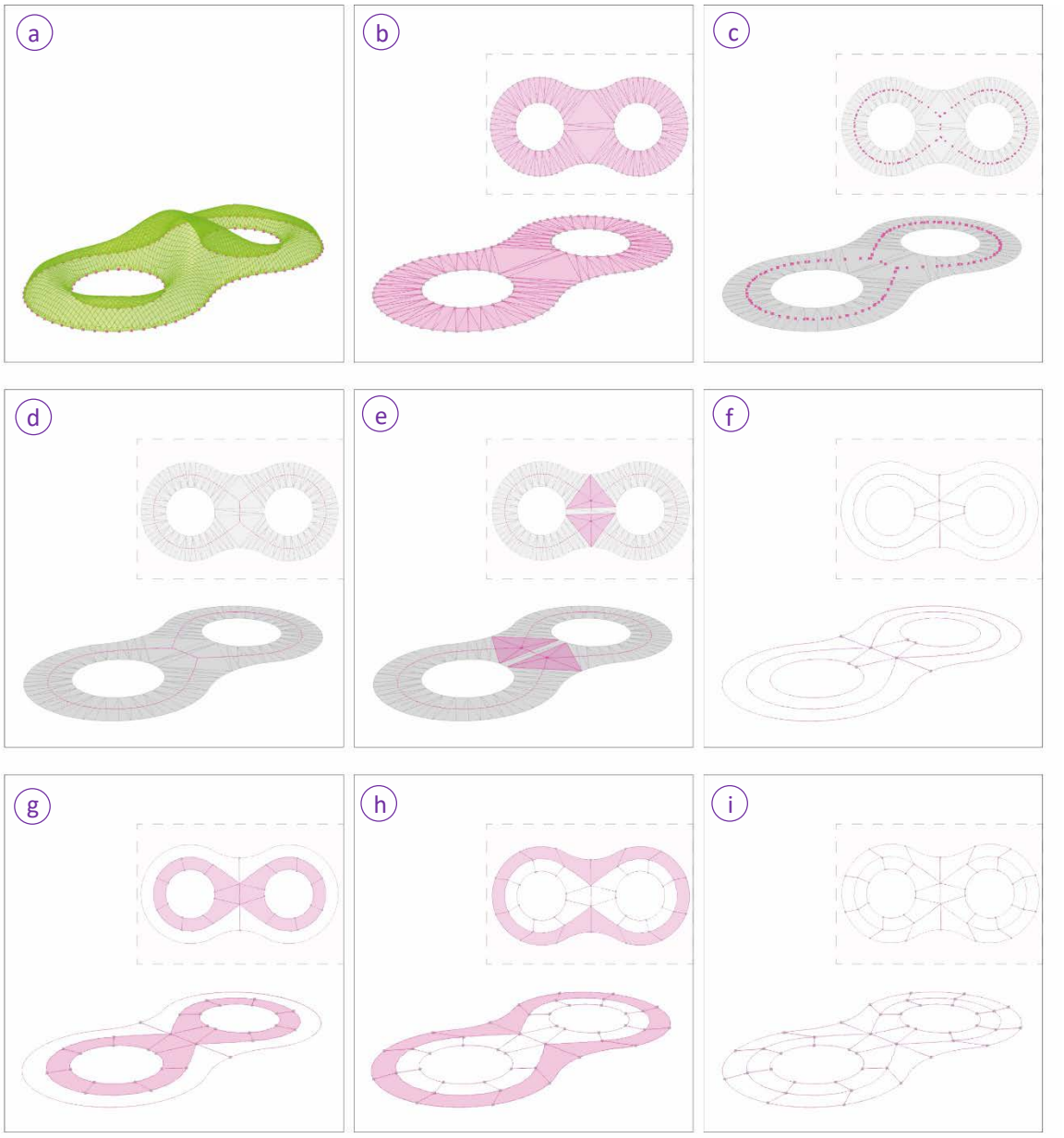

Figure 13: Different steps in constructing the topological diagram of a mesh.

However, some changes in the definition were necessary in order to subdivide the areas around the openings to prevent non-manifold faces. In contrast to the definition previously used for the complex shape discussed in Section 7.1.2, the number of divisions of these areas is now based on a variable parameter, rather than a fixed division. (Figure 13g-f) In this way the topological diagram can be modified into parts of equal length, which benefits the final panelization.

Based on this topological diagram the coarse mesh can be constructed followed by a subdivision and relaxation on the original shape. These steps are visualized in Figure 14. For these steps some adjustments related to the different type of input geometry were necessary, but the idea behind it is similar. Different components are used for extracting the boundary curves of the input mesh and for projecting points on meshes rather than Breps and surfaces.

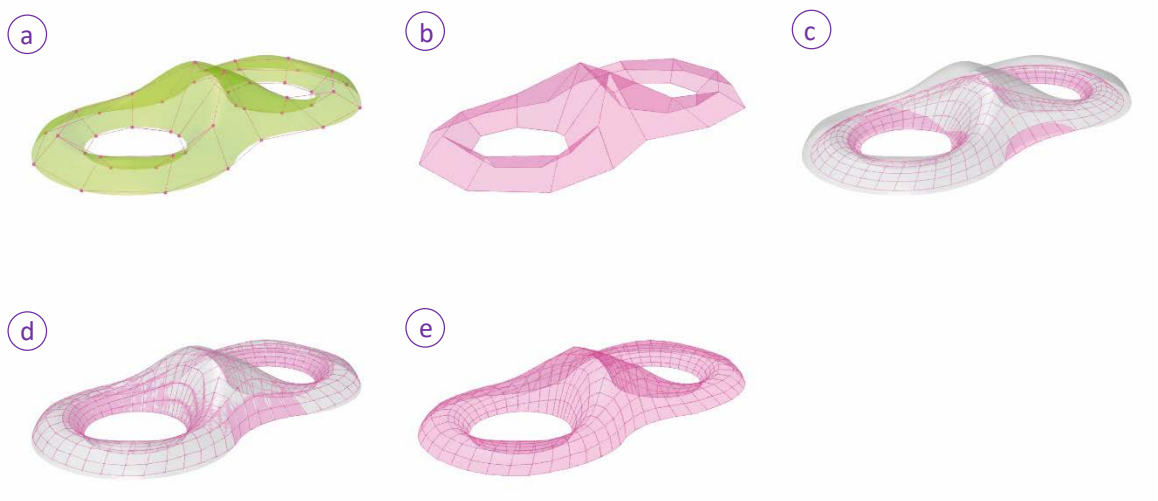

Figure 14: Different stages of mapping the coarse mesh onto the 3-dimensional input mesh, subdividing the coarse quad mesh and relaxing this mesh onto the original input mesh.

This quadrangular mesh, together with the input mesh, form the input for the redesign of the panels to developable surfaces discussed in Section 7.2.

7.1.5 Optimizing the grid

As described in Appendix A, the subdivision of panels, in particular the orientation of the grid, has an influence on the accuracy of the approximated shape. A higher accuracy to the original surface can be reached if the panelization is derived from the principal curvatures of the surface. (Liu et al., 2006) However, as concluded earlier, conjugate curve networks such as principal curves are not always suitable for panelization.

In the research of Winslow, Pellegrino & Sharma (2008; 2009) the authors tried to optimize a grid for structural performance by shifting the vertices, and therefore the edges, towards the optimum grid orientation. In theory the same thing could be done with the principal curvature directions instead of the optimum grid directions. One approach could be that the edges are forced to lie parallel to the principal curvature directions, as much as possible. The reason for this is to increase the approximation accuracy in the end result.

However, attempts to optimize the grid based on principal curvature directions have failed. First of all, because the parameterization directions based on the topology of the surface might deviate too much from the principal curvature directions. Therefore the aligning them with the principal curvature directions could lead to rugged edges in the mesh. But more importantly, the singular points in the mesh – which form the key element in this meshing method – are locations where more than 4 edges meet. Since there are only 2 perpendicular principal curvature directions at each location, these singular points form a problem in the optimization. Because of this there will no further optimizations of the grid implemented in this method.

7.2 Rebuilding the panel surfaces

The surface redesign can be seen as the process of rationalization. (Pottmann et al., 2014) As discussed before, this research will focus on the use of developable panels. The most simple method to create a developable surface is straightening one family of curvature lines, in order to create a zero Gaussian curvature. As described by Liu et al. (2006), developable surfaces consist out of an envelope of multiple planes, where all planes intersect with the surface along a straight line. These straight lines form the rulings of the surface. However, when dealing with a shape formed by multiple panels, each consisting out of a different surface, this method might lead to misalignment along panel edges since each panel is redesigned independently of its adjacent panels. These attempts are included in Appendix D. Due to the non-linear nature of developability one should mind that the tangent plane along a ruling must be constant.

Therefore a global approach is pursued in the method discussed in this section. This approach follows a method based on the research of Tang et al. (2016) and Gavriil, Schiftner & Pottmann (2018) as described in Appendix A. For this method the Gauss-image of the surface is flattened, which means reducing the Gaussian curvature to 0. This is done by forcing all surface normal vectors of the surface at the location of the sample points to lay parallel to the target plane of a panel.

7.2.1 Variational Shape Approximation

This approach is based on the methods described in Appendix A from the research of Tang et al. (2016) and Gavriil, Schiftner & Pottmann (2018). The surfaces of each panel are sampled at different points, these are called the sample points. Each panel consists out of the sample points corresponding to that panel. Gavriil, Schiftner & Pottmann (2018) introduce patches as well. In their method each patch consists out of the sample points of a panel, including the first row of points of the adjacent panel. It should be noted that a distinction is made between the panel and the patch corresponding to that panel. Having an overlap in the patches preserves the smoothness in the final shape. However, having these overlapping points is computationally very heavy since the normal vectors of the overlapping points are forced to lay parallel to two different planes. Besides this, the smoothness constraint of having this overlapping points in the patches might overrule the developability objective in the approximation.

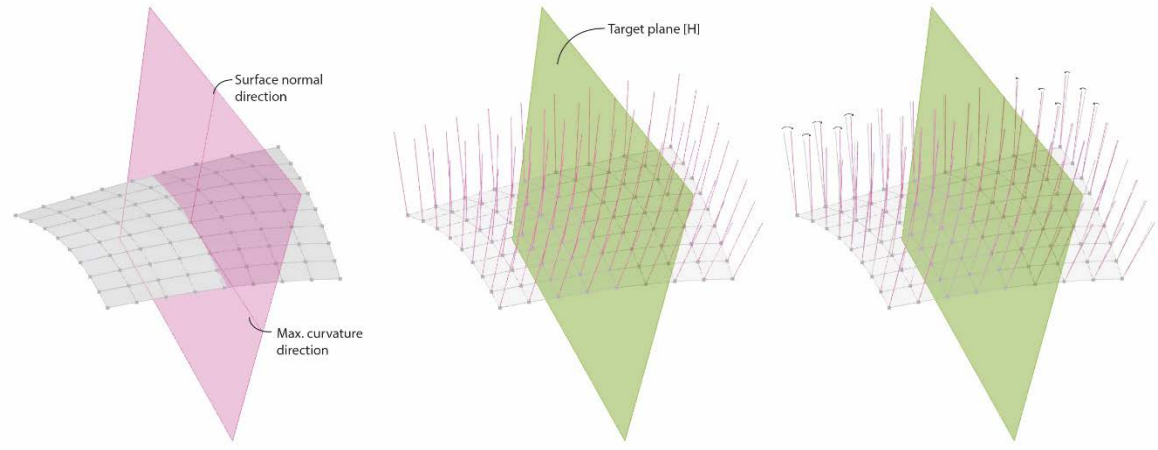

Figure 15: Visualization of the target plane of one panel (left), the surface normal vectors at the sample points in a panel (middle) and the normal vectors projected parallel to the target plane (right).

Therefore only the sample points that lay within the panel boundaries are used to create the patches in this research. This means that only the vertices located on the panel edges correspond to two different target planes since these are topologically connected to two adjacent panels. This is necessary in order to keep adjacent panels aligned. The goal of the method is to force all the normal vectors of a

patch to lay parallel to a target plane initialized in the centre of that panel in the direction of the maximum principal curvature at that location. (Figure 15) Positioning this target plane in the direction of the maximum principal curvature, straightens the family of curvature lines in the direction of the minimum principal curvature. In other words, straight rulings are created in the direction of the minimum principal curvature, so that the panel will follow the highest curvature and therefore the surface approximation will reach higher accuracies to the original shape.

It should be noted that a surface normal is a surface property at a certain point, and a property cannot be changed directly. In order to parametrize this model, the position of the sample points must be adjusted in order to modify the surface and therefore indirectly the surface normal vectors. It is important to treat the shape as a whole in order to keep the panels aligned and preserve overall smoothness in the shape. For this reason the shape must be modified as one mesh, where the individual surfaces of the panels are 'sampled' by subdividing the mesh to create the additional sample vertices.

7.2.2 Mesh subdivision corresponding to individual NURBS surfaces

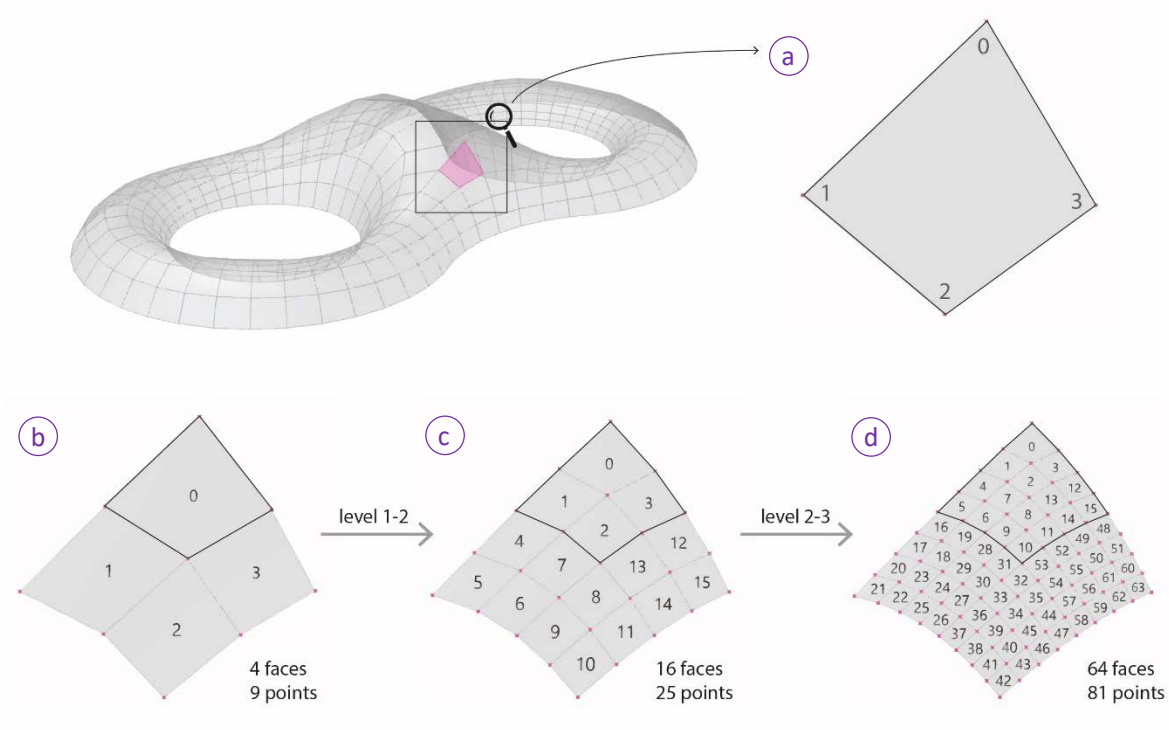

Figure 16: Subdivision of the mesh from the panelization algorithm. (a) represents a single panel, which is subdivided further with a Catmull-Clark subdivision to a level 3 division (b-d) where the mesh faces are sorted in a quad-tree like order.

As a result of working with a single mesh in the approximation, one should maintain the relation between the subdivided mesh faces to the original panel division. The Catmull-Clark subdivision subdivides the meshfaces in a quad-tree like structure as shown in Figure 16. In order to get a representative amount of sample points, a subdivision level of 3 is used, which gives us a sample point size of 81 vertices corresponding to 64 mesh faces for each panel. (Figure 16d)

Because of the nature of the Catmull-Clark subdivision, partitioning the list of mesh faces at a multiple of the number of faces per panel – 64 in the case of subdivision level 3 – provides lists of faces corresponding to the individual panels. These lists of faces are then used to retrieve the desired vertices for constructing the NURBS surfaces of each panel.

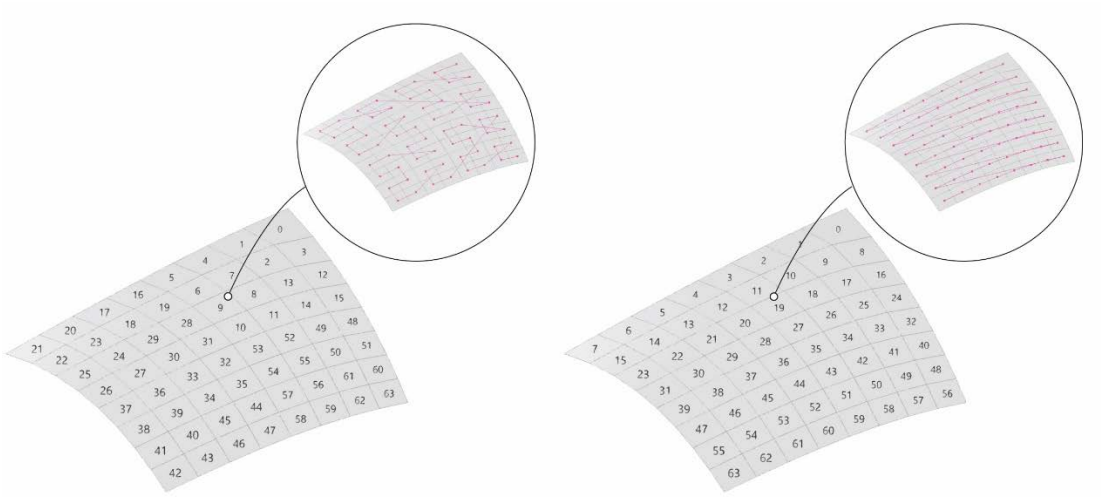

Figure 17: Converting the quad-tree order of faces (left) to a zigzag order (right) in order to select the vertices in the desired order per row.

Since the surface normal vectors at the location of the sample vertices are an input for the approximation, the panel surface needs to be evaluated at the location of their closest points on the surface. Therefore a NURBS surface needs to be constructed through the mesh vertices. For this the vertices need to be sorted in a zigzag order per row of vertices, as shown in Figure 18b. In order to develop an algorithm for sorting these vertices in the desired order, first the face-order needs to be modified from a quad-tree structure to a zigzag structure per row. (Figure 17) This process of face-sorting is manually implemented in the Grasshopper definition, only applicable for a mesh subdivision level 3, since this process is outside the scope of this research and a complex topic in itself.

When the faces are sorted in the desired order, the desired order of vertices is constructed by selecting individual vertex indices per mesh face. This algorithm is implemented in a python script of which the pseudo-code is explained below. It should be noted that the vertex order of each face after the subdivision is equal, as shown in Figure 16a.

A new list is created for the sorted vertices. The following code selects the vertices in the desired order, but only works after the mesh faces are sorted as shown in Figure 17.

```
For each face of the list of faces corresponding to a panel:
    If a face is the last face in a row of faces:
        Select vertices with index 0 and 1
    Else:
        Select only the vertex with index 0
```

The created list now only includes vertices 0-71 of the vertices shown in Figure 18b. Additional points from the last row of faces must be added in order to add vertices 72-80.

```
For each face in the last row of faces in a panel:
    If a face is the last face in the row of faces:
        Select vertices with index 3 and 2
    Else:
        Select only the vertex with index 3
```

The result is the list of 81 vertices sorted in the desired zigzag order for the construction of the NURBS surface.

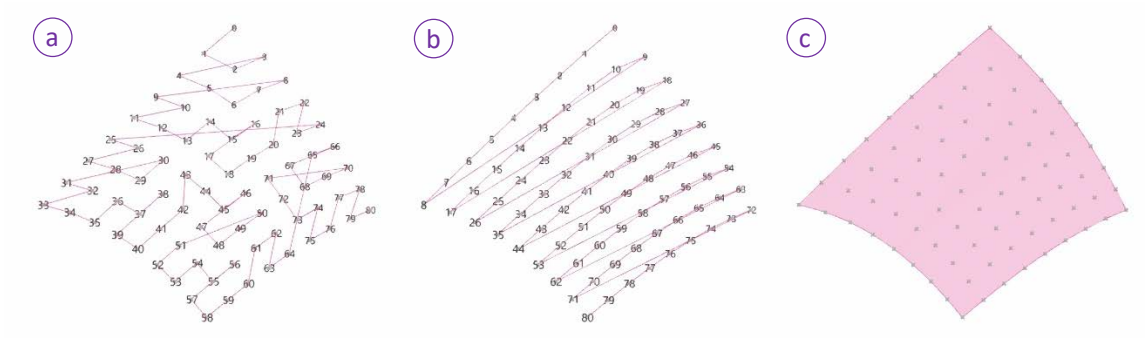

Figure 18: Order of mesh vertices after sorting of the faces (a). The desired order of the vertices from the algorithm described on the previous page. (b) An interpolated NURBS surface through the point cloud of the panel vertices. (c)

After the vertices of each panel are sorted in de desired order, a NURBS surface can be interpolated through the points. It should be noted that the 'NURBS *through* points' method is used instead of the 'NURBS *from* points' method. The latter uses the points as control points rather than points on the surface. The created surface represents the corresponding panel as an *untrimmed* surface.

7.2.3 The math behind the approximation

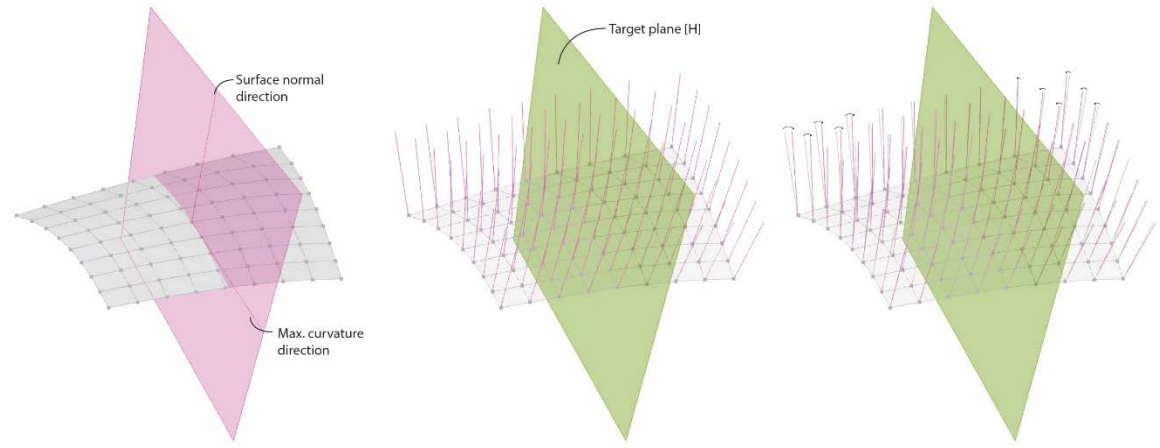

Figure 19: Visualization of the target plane of one panel (left), the surface normal vectors at the sample points (middle) and the normal vectors with their projection parallel to the target plane (right).

As mentioned before, the goal of the shape approximation is to force all normal vectors to lay parallel to the target plane. In order to do this, the definition of the projected normal vector must be derived. Based on Figure 20b it can be concluded that vector [u] is equal to the summation of its horizontal component [h] and its vertical component [v] relative to the target plane. This means that the projection of vector [u] on the target plane [h] is equal to vector [u] subtracted by its vertical component [v]. Since this vertical component [v] is equal to the projection of [u] on the normal vector of the target plane [u_p], the equation can be rewritten as stated in Equation 1.

$$\begin{aligned} \vec{u} &= \vec{v} + \vec{h} \\ \vec{h} &= \vec{u} - \vec{v} \\ \vec{h} &= \vec{u} - \overrightarrow{u_p} \end{aligned} \tag{1}$$

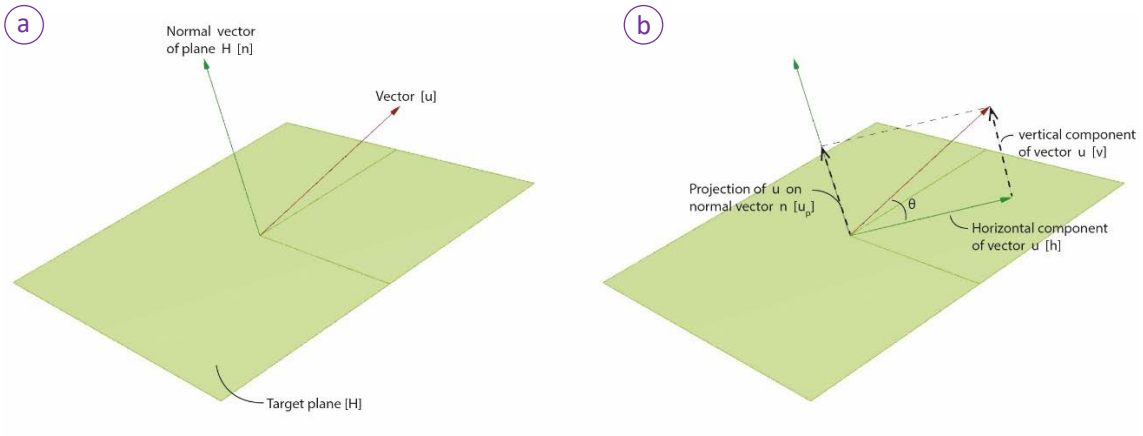

Figure 20: (a) A visual representation of the target plane with corresponding normal vector and the vector to be projected. (b) As well as a representation of the projection of the vector onto the plane with the parameters corresponding to the derived equations.

The projection of a vector [u] onto another vector [v] is something that can be derived from the following equations.

$$\overrightarrow{u_p} = |u| \cdot \cos(\theta) \cdot \frac{\vec{v}}{|v|} \tag{2}$$

$$\cos(\theta) = \frac{\vec{u} \cdot \vec{v}}{|u| \cdot |v|} \tag{3}$$

Substituting Equation 3 into Equation 2 provides us with the following.

$$\overrightarrow{u_p} = |u| \cdot \frac{\vec{u} \cdot \vec{v}}{|u| \cdot |v|} \cdot \frac{\vec{v}}{|v|} \tag{4}$$

In Equation 4, $|u|$ can be streaked away against each other which provides us with the following.

$$\overrightarrow{u_p} = \frac{\vec{u} \cdot \vec{v}}{|v|} \cdot \frac{\vec{v}}{|v|}$$

$$\overrightarrow{u_p} = \frac{\vec{u} \cdot \vec{v}}{|v| \cdot |v|} \cdot \vec{v}$$

$$\overrightarrow{u_p} = \frac{\vec{u} \cdot \vec{v}}{|v|^2} \cdot \vec{v} \tag{5}$$

Equation 5 provides the definition for projecting a vector [u] on another vector [v]. In the current objective [v] represents the normal vector of the target plane [n]. Substituting vector [v] of Equation 5 with the normal vector of the target plane [n] and substituting this new equation into Equation 1 gives us the following formula.

$$\vec{h} = \vec{u} - \frac{\vec{u} \cdot \vec{n}}{|n|^2} \cdot \vec{n} \tag{6}$$

Equation 6 provides the definition of the projection of vector [u] on the target plane with only two variables being the original vector [u] and the normal vector of the target plane [n].

7.2.4 Objectives for the shape approximation

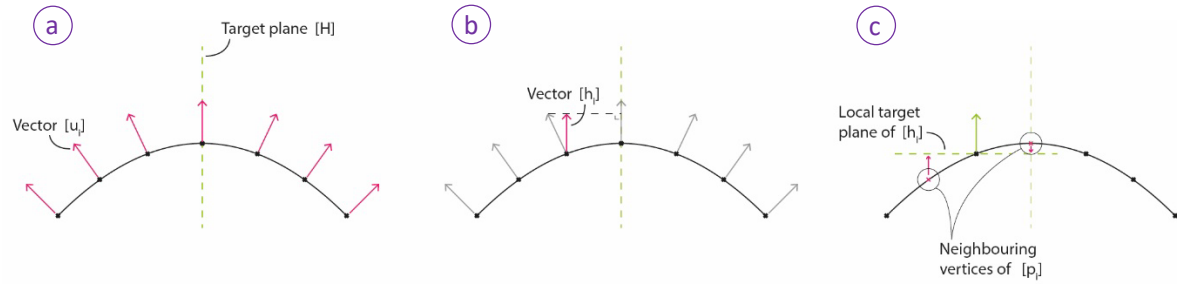

Figure 21: Retrieving the surface normal at each sample point p_i (a), constructing local target planes in each vertex based on their projected vector [h_i] (b) to attract its neighbouring vertices to (c).

As discussed earlier the goal of the surface approximation is to force all surface normal vectors at the sample points parallel to the target plane. This goal is now defined in Equation 6. However, a surface normal is a surface property at a certain point and a property cannot be changed directly. The slope and curvature of a surface at a certain point is dependent on the relative position of its neighbour vertices, since the surface is interpolated through these vertices. Therefore a local target plane is initialized in each sample point, with a z-direction in the direction of projected vector h_i, where each 'neighbourhood' of vertices is pulled towards. Figure 21 schematizes this principal, whereas Figure 22 visualizes the application on a single vertex of a mesh representing a 3-dimensional panel.

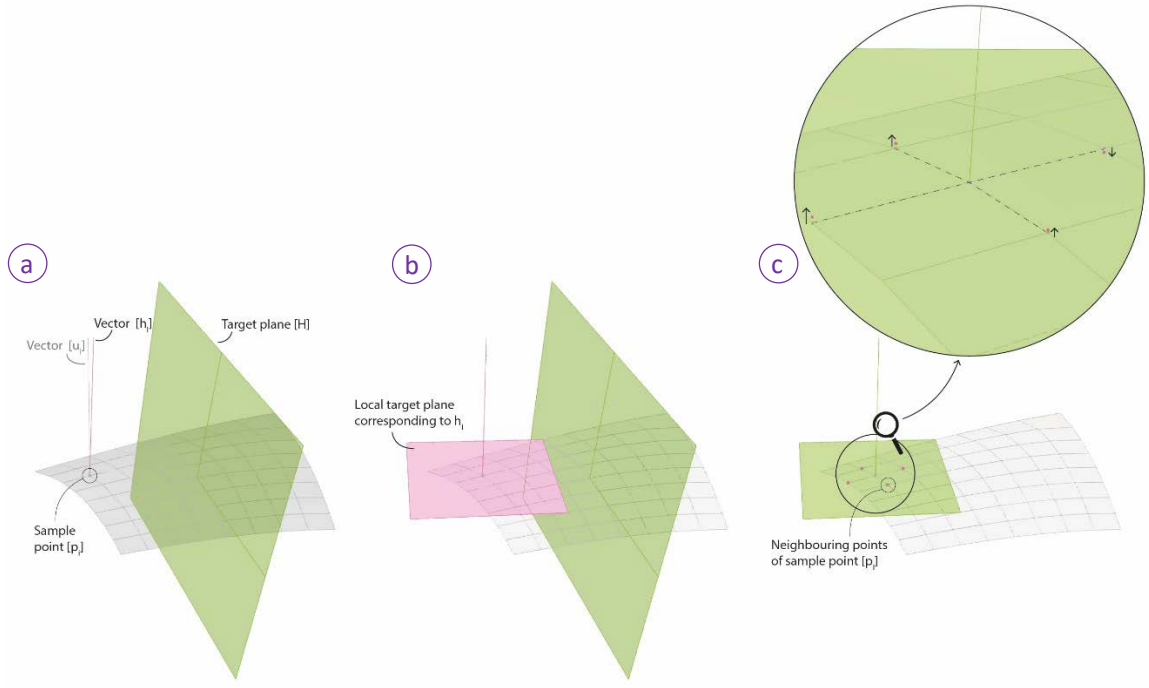

Figure 22: Same principle as Figure 21 on a 3-dimensional panel. Retrieving the surface normal at each sample point p_i and projecting them on Target plane *H* (a), constructing local target planes in each vertex based on their projected vector [h_i] (b) to attract its neighbouring vertices to (c).

In order to run the shape approximation the methodology is implemented in a Grasshopper definition using the Kangaroo2 plug-in. The following Objectives are included in the dynamic relaxation:

- *Points on Plane (OnPlane):* For this component a neighbourhood of points is collected, corresponding to each sample point. These neighbouring points can be retrieved from the mesh topology. For each neighbourhood of points a local target plane is set as described above.

- *Points on Mesh (OnMesh):* For this component all mesh vertices, as well as the mesh itself, is inserted. This component will try keep a point on the mesh, which is necessary in order to prevent high deviations from the original shape.
- *Edges as Springs (Length (line)):* This component converts al mesh edges to springs, which will try to keep the edges at their original length.
- *Anchor points (Anchor):* This component will try to keep all the points at their original location.

The goal-objects mentioned above provide the necessary input for increasing the developability of the panels, but an additional goal-object related to the production of the final sandwich panels is necessary. All edge curves should be planar so that all rib-elements for the sandwich structure can be cut out of planar steel sheets.

- *Planarize edge curves (CoPlanar):* For this component all vertices corresponding to each panel edge are retrieved and this component will try to make the points co-planar.

Together with the previously mentioned Objectives, this forms the input for the dynamic relaxation. Each objective is assigned a different strength related to the priority it has. The objective for increasing the developability and the objective to planarize the edge curves have a higher importance than the other objectives and therefore a higher relative strength is assigned to them.

7.2.5 Results of the shape approximation

Besides the mesh vertices and the normal vector of the target plane [n], the normal vectors of the panel at the location of each mesh vertex (i.e. sample point) [u] is also an input for the objective of increasing the developability. In order to get accurate curvature results, the curvature of the NURBS surface of the panel is measured at parameters corresponding to the location of the mesh vertices. (Figure 23c) Vectors [u_i] are therefore also based on the curvature of the NURBS surface (Figure 23b) rather than an average of the mesh (Figure 23a).

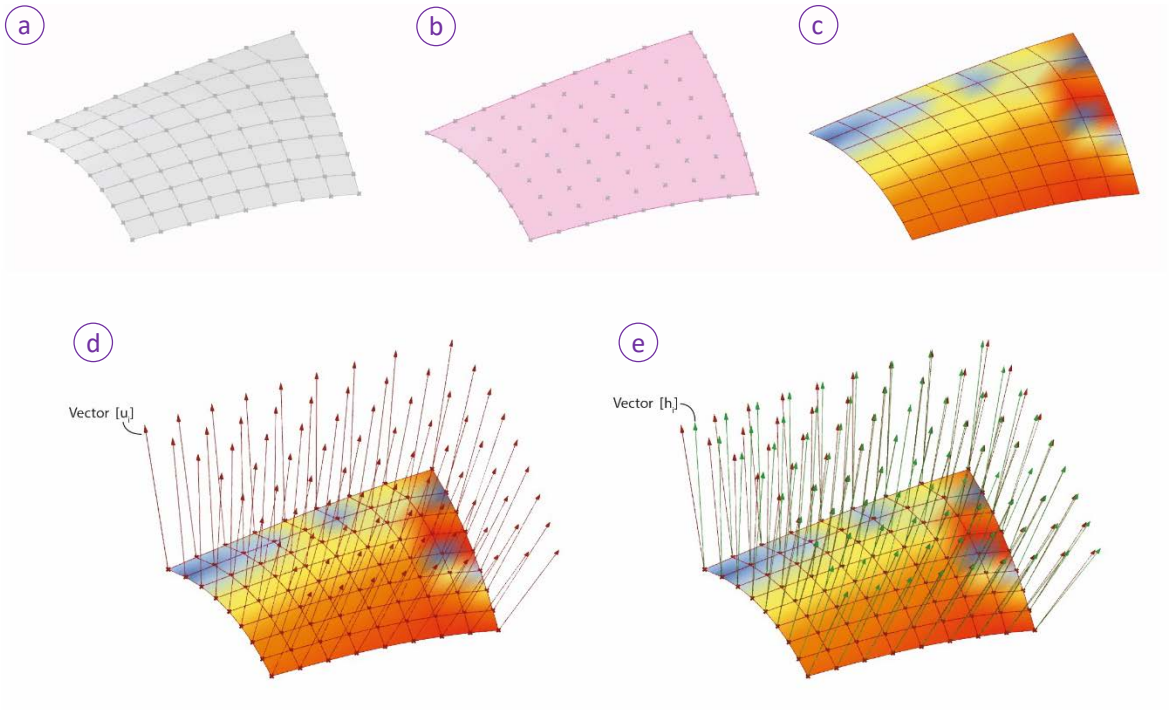

Figure 23: Visualization of the input geometry (a + b), curvature analysis (c), surface normal vectors (d) and target vectors (e) before the dynamic relaxation.

Table 1: Gaussian curvature and statistics of the original panel surface.

Assigned strengths	Average Gaussian curvature	Standard Deviation	Range in curvature
OnPlane: 0 *OnMesh: 0* *Length(line): 0* *Anchor: 0* *CoPlanar: 0*	0.0092	+/- 0.0139	-0.0090 to 0.0263

As mentioned before, the objectives with a higher priority should be assigned relatively higher strengths than others. Therefore the CoPlanarity component, which forces the edge curves of a panel surface to planar curves, has a relatively high strength in order to ensure the sandwich structure is able to be produced with planar ribs in the structure. Besides this, different combinations of strengths for the OnPlane component, which increases the developability of the panel surface, are tested as well. Next to a fixed strength, which is equal for each local target plane, a possible variable strength is investigated. This variable strength is related to the average distance of a neighbourhood of points to that local target plane. All average distances will be reparametrized and multiplied by this variable force strength. The larger the initial average distance to the local target plane, the higher the strength of the component for that specific target plane will be.

Table 2 provides results for different combinations of fixed- as well as variable strengths, all visualized in Figure 24a-c. It should be noted that a lower average Gaussian curvature does not necessarily mean a higher developability of the panel, one should pay attention to standard deviation and the range in Gaussian curvature as well to judge whether the approximation reaches successful results.

Table 2: Gaussian curvature and statistics of the panel surface with different settings for the dynamic relaxation. F: Fixed force and V: Variable force. These results correspond respectively to Figure 24a-c.

Assigned strengths	Average Gaussian curvature	Standard Deviation	Range in curvature
OnPlane: F-1 *OnMesh: F-1* *Length(line): F-1* *Anchor: F-1* *CoPlanar: F-50*	0.0002 (-4041%)	+/- 0.0235	-0.0923 to 0.0259
OnPlane: V-1 *OnMesh: F-1* *Length(line): F-1* *Anchor: F-1* *CoPlanar: F-50*	0.0033 (-176%)	+/- 0.0152	-0.0788 to 0.0218
OnPlane: V-5, F-1 *OnMesh: F-1* *Length(line): F-1* *Anchor: F-1* *CoPlanar: F-50*	-0.0033 (-377%)	+/- 0.028	-0.0084 to 0.0435

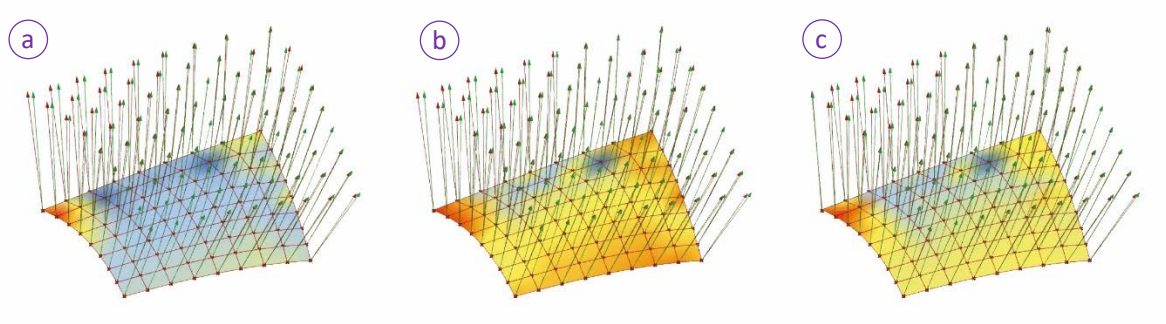

Figure 24: Visualisation of the approximation results shown in Table 2. In the figure red corresponds to a negative Gaussian curvature, yellow to a neutral (i.e. close-to zero) Gaussian curvature and blue to a positive Gaussian curvature.

Although full developability is not reached with the current settings, it can be stated that the overall curvature in the panel is reduced in the case of a single panel. In Figure 24c a variable force per plane is introduced, which leads to better results compared to the previous settings. With these settings an approximation is done for a group of panels taken from the entire mesh. These results and visualisation of the results are shown respectively in Table 3 and Figure 25a-b. According to Table 3 an overall increase in curvature is expected, but the visual results in Figure 25b show that mayor part of the panels show a decrease in curvature towards zero Gaussian curvature. The problems arise towards the panel edges, these are the locations where the sample points share two different target planes in the objective.

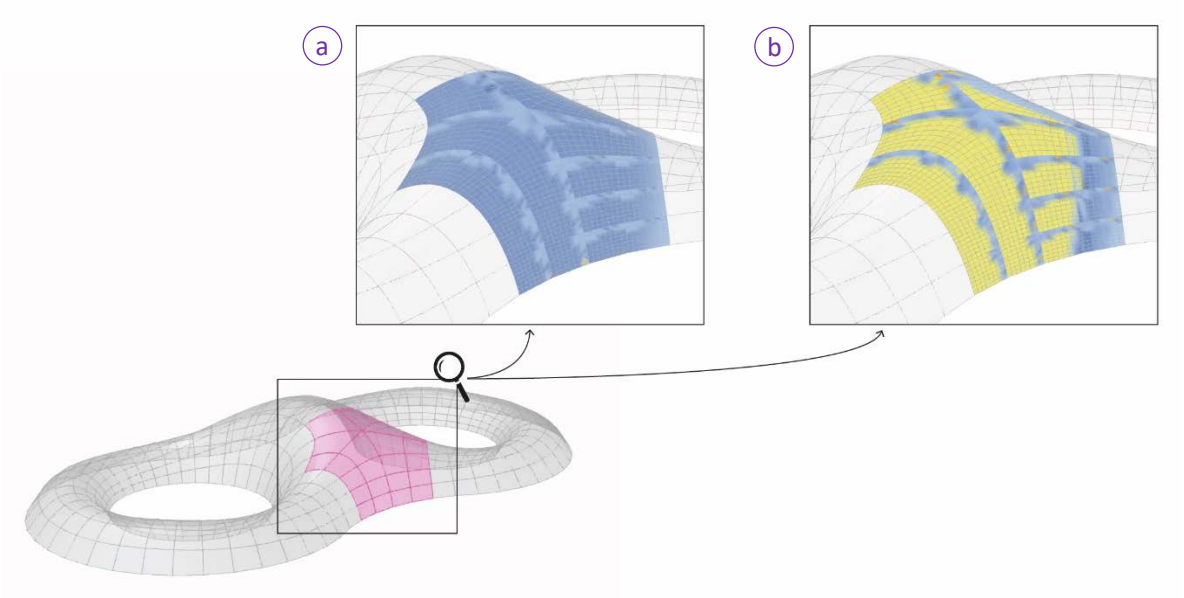

Figure 25: Visualisation of the approximation results shown in Table 3. In the figure red corresponds to a negative Gaussian curvature, yellow to a neutral (i.e. close-to zero) Gaussian curvature and blue to a positive Gaussian curvature.

Table 4: Gaussian curvature and statistics of the panel surfaces before and after shape approximation. F: Fixed force and V: Variable force. These results correspond respectively to Figure 25a-b.

Assigned strengths	Average Gaussian curvature	Standard Deviation	Range in curvature
OnPlane: 0 *OnMesh: 0* *Length(line): 0* *Anchor: 0* *CoPlanar: 0*	0.0092	+/- 0.0139	-0.0090 to 0.0263
OnPlane: V-5, F-1 *OnMesh: F-1* *Length(line): F-1* *Anchor: F-1* *CoPlanar: F-50*	0.0675	+/- 0.0502	-2.8127 to 9.5016

7.2.6 Limitations of the method

Although full developability is not reached with the current settings as mentioned before, it can be stated that the overall curvature in the panel is reduced. In Figure 24c a variable force per plane is introduced, which leads to better results compared to the previous settings. This variable force however is related to every local target plane in a sample point (Figure 21c), which means every point in a neighbourhood of points is pulled towards the corresponding plane with the same force. Instead of exerting a higher force on an entire neighbourhood of points, future improvements could base this variable strength on individual points rather than the local target planes.

This method increases the developability locally, measured at each sample point. This does not necessarily mean developability in the entire panel can be accomplished. In order to increase the accuracy of the results, one might use a larger sample point size (i.e. higher level of subdivision) for each panel in order to increase the amount of control points of the surface. Implementing higher levels of subdivision does however demand solutions for automatic face-sorting from the quad-tree order to a zigzag order as shown in Figure 17.

For a neighbourhood of panels, problems arise near the panel edges, where the vertices share two different target planes. Approaching the global shape with developable stripes, where groups of panels share common target planes, might reduce this problem. (Figure 26) This could be an interesting topic for future research.

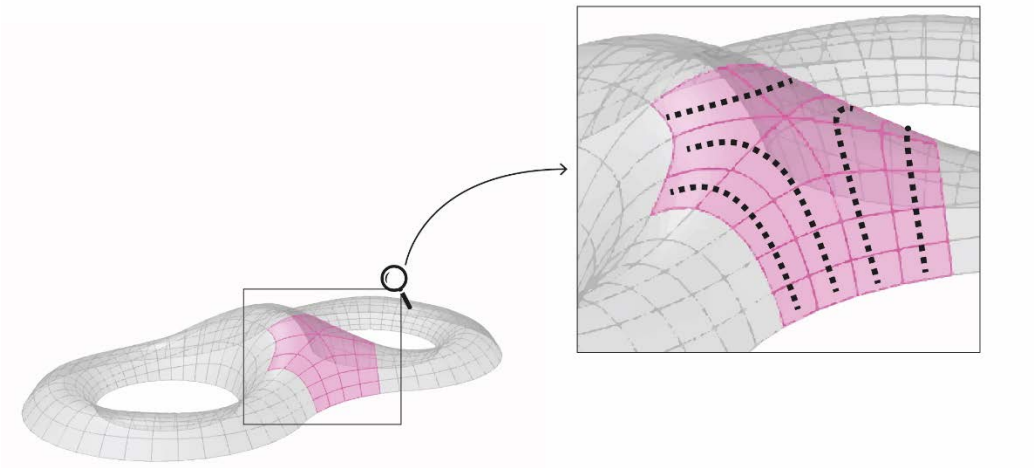

Figure 26: Grouping panels into stripes in order to create common target planes.

7.3 Validating the structure

There are many ways to optimize a grid for structural performance, such as shape optimization, size optimization and topology optimization (Grande, Imbimbo & Tomei, 2018). For the purpose of this research this respectively means changing the orientation of the grid, changing dimensions of the grid and beam elements, and changing the type of grid. Winslow, Pellegrino & Sharma (2008; 2009) developed an algorithm to change the orientation of the grid towards the optimal direction for structural purposes. However, the design of the grid has a mayor influence on the accuracy of the surface approximation as explained in Section 7.2.2 and 7.2.3.

Changing the type of structural grid could benefit the structural performance as well. Mensil et al. (2017b) describe in their research a method to convert quad grids to kagome grids. (Section 6.2.3) According to their research kagome grids outperform quad grids when compared on structural efficiency. This can be explained by the fact that there are grid elements in more than two directions, which reduces the bending moment in the beams because more beams are loaded axially. Besides this, the triangulated elements in the grid gives more geometrical stiffness so the stiffness of the grid does not rely only on the bending stiffness of the nodes.

However, based on the used method to initialize a quad grid on a topologically complex surface, some valence 5 nodes arise in de model. This means at some nodes five panels meet. Selecting quads in a checkerboard pattern and modifying them to kagome cells cannot be done near these valence 5 nodes. For the purpose of this research, the corners of the quads will be stiffened by simply triangulating them with additional rib elements. This definition will therefore serve as a preliminary validation for the structural performance in the design stage, in order to provide and estimation for the minimum sheet thicknesses, rib thicknesses, rib heights and possibly the location of the stiffeners in a panel.

This chapter is subdivided in different paragraphs, the first paragraph explains the objectives for the structural analysis. In the second paragraph a definition is set up for creating the sandwich panels, initializing the elements for the structural calculations and validating the analysis. This is done using a relatively simple vault structure, divided into quadrangular panels. For the validation of the definition a simpler model is necessary in order to check whether the model is correctly set up.

7.3.1 Objectives for the structural analysis

For the validation of the structure, Ultimate Limit States (ULS) as well as Serviceability Limit States (SLS) will be taken into consideration. Next to utilization of the shell elements and deformation of the entire structure, a buckling analysis will be included as well. This because it is an important aspect for grid shells. By including a buckling analysis in the design stage of the structure rather than just a verification at the end, the design of the grid could be adjusted rather than just increasing the cross-sections in the grid. (Grande, Imbimbo & Tomei, 2018; Winslow, Pellegrino & Sharma, 2008) Parameters in this validation consist out of rib thickness, rib height, sheet thickness and the position of the corner stiffeners. The rib height is directly related to the total panel height.

The structural analysis will be performed using the Grasshopper plug-in Karamba3D, so that the whole process can be kept within the same parametric environment. As mentioned before, it is important to validate the Grasshopper definition and Karamba structural analysis before the results can be trusted. A part of the model will be inserted into the definition in order to check if the number of structural elements is correct, all vertices align, loads are attached correctly and support reactions add up.

7.3.2 Setting up the definition

Creating the element geometries

As mentioned in the introduction of this chapter a simple barrel vault geometry is used for setting up the Grasshopper definition. Four different element geometries are used in the Karamba3D calculation of which the first two are the bottom- and top sheet geometries representing the curved steel sheets of the structure. The third element geometry consists out of the ribs of the panels and the fourth and last consists out of the corner stiffeners. These stiffeners can be seen as additional ribs in the panel.

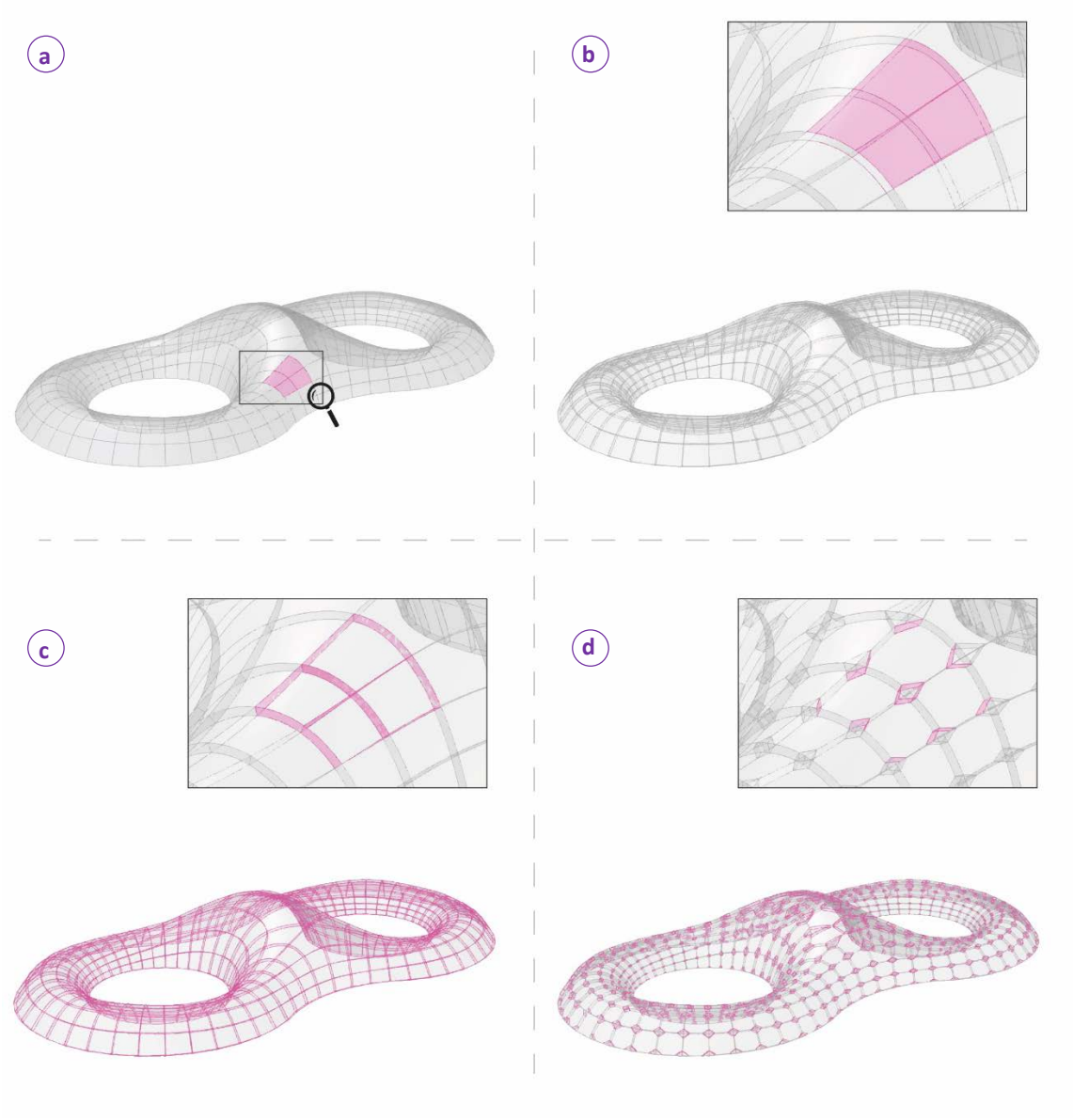

Figure 27: Creating the four different element geometries for the structural validation in Karamba3D.

However, the output of the previous step should first be converted to the desired element geometries representing the proposed sandwich structure. The starting point of this Grasshopper definition therefore is a quadrangular panelization followed from the rebuilding of the surface. Figure 27 visualizes the steps for creating the different element geometries that are necessary.

a. After rebuilding the surfaces based on the created quadrangular grid, a 1-dimensional list of surfaces representing each panel is the output. Each surface on its own will be converted to a sandwich panel.

b. The first step is to give every surface an offset equal to the parameter of the rib height of the panels. The two layers correspond to the top- and bottom sheets of the panel and are organized in a tree structure where each branch corresponds to a panel.
c. The edges of the top- and bottom surfaces are extracted and lofted in order to create the rib geometries. Since these top- and bottom surfaces are sorted in different branches for each panel, each panel will have four surfaces that represent the four ribs. Adjacent panels therefore have the same rib geometry where they meet, but these double ribs are necessary because each panel is surrounded by four ribs as explained in Section 7.1.
d. In order to provide some lateral stiffness in the panels, the corner stiffeners are constructed. This is done by evaluating each edge curve at length X and the total curve length minus X. This will create 2 points on each edge curve, so 8 points per panel sheet all sorted along the boundary curve of the sheet. Each point is connected to its closest point on the adjacent edge by shifting the list of points by 1. This is done for the top sheet as well as the bottom sheet. These lines are then projected on the sheet surfaces and lofted to create the additional corner ribs, referred to as corner stiffeners.

Meshing the element geometries

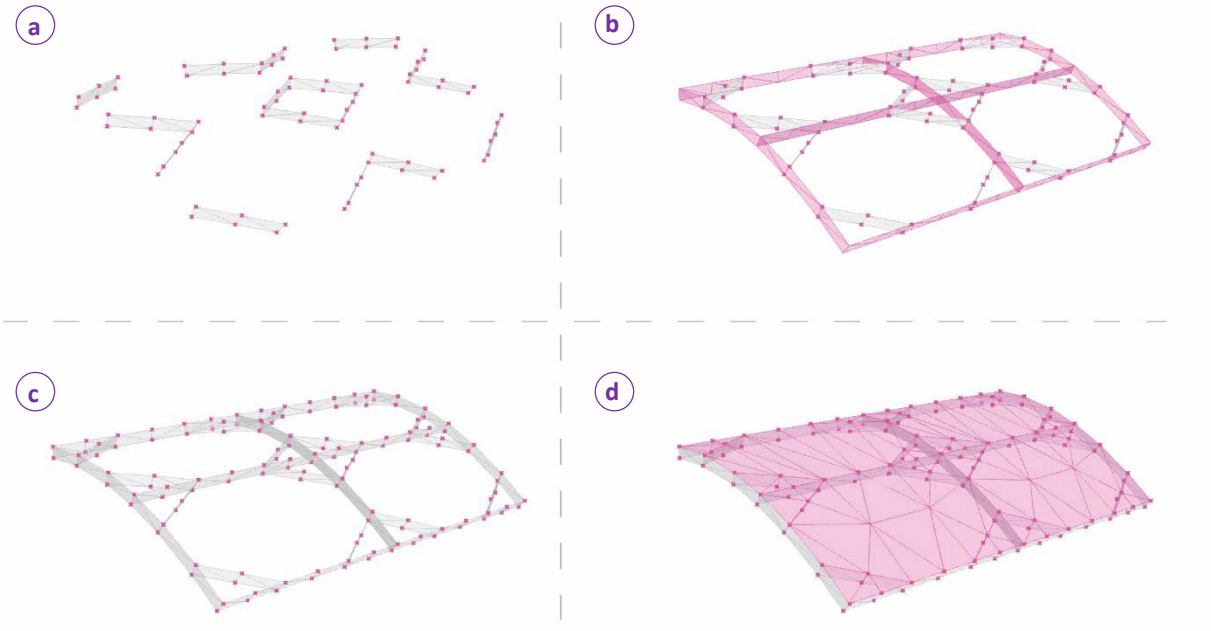

Figure 28: Initializing the meshes for each element geometry.

The constructed element geometries need to be converted to meshes for the structural analysis with Karamba3D. It should be noted that for each shared edge, the vertices of both elements meeting there must align exactly. If this is not the case, forces cannot be transferred from one element to another, as if they are disconnected. The meshing definition is tested on a small part of the barrel vault (e.g. 4 panels), in order to be able to check the results. The steps for the meshing of the different elements are visualized in Figure 28 From each meshing step the vertices are stored and included in the meshing of the next element. First the corner stiffeners are meshed (Figure 28a), as mentioned before the vertices of this mesh are stored and included in the meshing of the ribs (Figure 28b). This ensures that the meshing algorithm constructs vertices at the location where the corner stiffeners meet the ribs of the panel. Consequently the new vertices from the mesh of the ribs are stored as well (Figure 28c) and included in the meshing of the top- and bottom sheets (Figure 28d). For this the 'Mesh Breps'-component from Karamba3D is used, since this component has a build-in input for inclusion points. This component will generate a vertex at the inclusion points, as long at the shortest distance between the point and the Brep is smaller than 0.00001m. (Preisinger, 2018)

Since calculating these inclusion points based on a large point cloud and multiple Breps is computationally demanding, all this information is stored in different branches for panel. This speeds up the meshing significantly.

Assembling the model

The output of the meshing provides the four different element geometries for the analysis. The bottom- an top sheets, rib elements and corner stiffeners. For these geometries the supports, loads, cross-sections and materials are defined next.

Supports:

For the supports the mesh vertices from the top- and bottom sheet meshes are retrieved. In order to speed up the calculation the mesh vertices from the ribs and corner stiffeners are left out. This will however not form a problem as Karamba recognises that they are the same because of their coordinates. For the vertices for the top- and bottom sheet meshes the lowest Z-value is retrieved and all vertices with a Z-value equal to this value are selected as supports. Other ways of selecting supports could be included as well, but for buildings and pavilions the supports are usually at the lowest points. The supports are given 3 degrees of freedom and are only fixed in the 3 translational directions.

Loads:

Three different loads are included in the definition. A gravity load (permanent load), a vertical live load and a horizontal live load (both live loads). The vertical live load represents in the worst case scenario snow loads in winter. Derks (2012) summarizes the Eurocode for snow loading, the most negative case would be a flat roof. For his calculation he uses a characteristic value for the snow loading of 0.7 kN/m^2 and he reduces it with a form factor for a flat roof of 0.8 which consequently gives a value of 0.56 kN/m^2 as snow load. This value will be used in this analysis as a projected Mesh Load. The horizontal live load represents the wind load as a simple projected load colliding with the first panels it encounters. For this an average value of 0.8 kN/m^2 is used for positive- as well as negative wind pressure on the structure. For the Ultimate Limit State (ULS) analysis all permanent loads will be multiplied with a safety factor of 1.2 and all live loads with a safety factor of 1.5.

Cross-sections:

Since the purpose for this definition is to provide a validation of the structure in the design stage rather than a full optimization, only two different cross-sections are assigned to the geometries. The top- and bottom sheet elements will be assigned a constant thickness and the rib- and corner stiffener elements will be assigned a constant thickness.

Materials:

The purpose of this research is to provide a method for steel structures, and as described in Section 7.1, only steel is used. The default material for this structural analysis is set to S235 Steel.

Validation of the model

At this point all inputs necessary for the structural analysis are set and they can be assembled. First a simple first order analysis is done in order to check whether the model is set up correctly. For this the AnalyseThI component of Karamba3D is used. The total weight, distributed loads for each panel and total vertical reaction force are retrieved from the analysis as well as manually calculated in order to compare the results.

Total weight:

The total weight of the structure can be manually calculated by first retrieving the areas of all top- and bottom sheets, multiplying it with the sheet thickness and the density of the steel.

Secondly by retrieving the areas of the rib- and corner stiffener elements and multiplying this with the rib thickness and the density of the steel. These values added should be equal to the total weight given as output of the first order analysis of Karamba. A comparison between these results is made for the barrel vault geometry from the example, the exact numbers are shown in Table 4. There is only a small difference (0.07%) in total weight, which is most likely due to the meshing. The manual calculations are based on the NURBS surfaces of the geometry as input, while the Karamba total weight is based on the input meshes. These meshes are an approximation of the NURBS geometry and could deviate slightly in area, and therefore influence the total weight. However, it can be concluded that all elements are included in the analysis, as well as the double ribs occurring with adjacent panels.

Table 5: Comparison of the total weight from the analysis and manual calculation based on the barrel vault geometry from the example.

	Total weight of the structure
Manually calculated	45 952 kg
Retrieved from the Karamba AnalysisThI	45 920 kg
Absolute difference	32 kg
Relative difference	***0.07 %***

Distributed loads:

In order to check whether the vertical projection of the snow loading is correctly executed, the resultant force of the projected Mesh Loads from Karamba and the resultant force of the projected distributed load that is manually calculated, are compared for a random sample of panels. The comparison results of 4 random chosen panels is shown in Table 5. It can be concluded that the vertical projection of load is working properly.

Table 6: Comparison of the resultant vertical force from the Karamba MeshLoads component and manual calculations regarding the vertical live loads, based on the barrel vault geometry from the example.

Resultant forces [panel index]	**[0]**	**[37]**	**[84]**	**[118]**
Manually calculated	2.71	4.70	3.85	3.34
Retrieved from the Karamba MeshLoads	2.71	4.7	3.85	3.34
Absolute difference	0.0	0.0	0.0	0.0
Relative difference	***0.0 %***	***0.0 %***	***0.0 %***	***0.0 %***

Total vertical reaction force:

The last part of validating the model is done by decomposing the model after the analysis, retrieving the reaction forces and deconstruct these reaction forces to get the vertical components from it. These are mass added and compared with the result from the manual calculation. It should be noted that in this case, the gravity load, as well as the vertical live load is included. The comparison is shown in Table 6. There is a difference of 0.32 kN, which is converted to kilograms a difference of 32 kg. This is again the difference in total weight, caused by the meshing.

Table 7: Comparison of the total vertical reaction force from the Karamba analysis and manual calculation based on the barrel vault geometry from the example.

	Total vertical reaction force
Manually calculated	762.00 kN
Retrieved from the Karamba AnalysisThI	762.32 kN
Absolute difference	0.32 kN
Relative difference	***0.04 %***

Second order and buckling analysis

Now the model is proved to be working properly, a second order analysis is executed in order to determine the second order effects for the highest compressive forces in the structure. This component includes a buckling analysis. As mentioned in the introduction of this chapter, buckling is an important phenomenon to take into consideration for (grid)shell- structures. (Grande, Imbimbo & Tomei, 2018; Winslow, Pellegrino & Sharma, 2008) Even if the structure fulfils all requirements related to the Ultimate Limit States (ULS) and Serviceability Limit States (SLS), the system could still fail because of buckling. This is because the in-plane forces in shell elements change the behaviour of the elements under transverse load. Where tensile forces would have a stiffening effect, compressive forces have a softening effect. (Preisinger, 2018)

Although the cross-section optimization component from the Karamba3D library includes buckling effects in its algorithm, no cross-section optimization is included in the definition since only 2 different constant cross-sections are used in the scope of this research. The Buckling modes are therefore calculated with the 'Buckling Modes' component from the Karamba3D library. This component takes the model from the AnalyseThII (i.e. second order analysis) as input. Another important input is the number of buckling modes to be calculated. (Preisinger, 2018)

In general a Buckling Load Factor above 1.0 means no buckling occurs in the structure. However, this result is based on a perfect geometry and surface quality of the elements. In reality this is almost impossible to reach since there might be small deviations in geometry due to the production and scratches and dents from transportation and assembly. These imperfections lead to sensitive spots in the structure. Hoogenboom (n.d.) discusses a knock-down factor in order to compensate for imperfections in the elements. As a rule of the thumb he proposes to use the following knock-down factor.

$$C = \frac{1}{6} \tag{7}$$

The buckling factors will be multiplied with this knock-down factor, which consequently means that the buckling factor should be six times as high in order to fulfil the requirements. Therefore a Buckling Load Factor above 6.0 is required after compensating for imperfection in the elements.

As mentioned before the number of buckling modes forms an important input for the Buckling Modes component. By default this number is set to 1. (Preisinger. 2018) However, in asymmetric structures there is a possibility that one specific panel buckles given the maximum compressive force of all load cases, while all other panels do fulfil the requirements for buckling. In this case it can be considered to reinforce that specific panel only, rather than increasing the cross-sections in the whole structure. By setting the number of Buckling Modes to a higher number, not fewer than 5, the performance of the weakest panels can be evaluated. Since the Buckling factors are sorted in ascending order, it can be concluded whether a single panel, a few panels or most of the structure is buckling. Based on this it can be decided to respectively reinforce a single panel, a few panels or the complete structure.

8 Conclusion

The main research question based on the objective of this research was formulated as follows:

> *"How can free-form steel shapes be approximated by individual panels in order to prepare for the production?"*

This main question is answered by splitting it into several smaller parts, of which the results will be briefly summarized.

What are the restrictions and limitations of the production and how do they affect the panel shapes and sizes? – Different production methods have been discussed, ranging from traditional to new methods. There are a lot innovative new methods under development, which all demand new, costly machinery. However, even these innovative methods have their own limitations and inaccuracies such as a limited panel sizes, limited thicknesses (< 2 mm), potential dents in the finishing of the surface, but most importantly: they still need to deal with the springback effect of the material. Closed loop forming methods reduce the springback of the material significantly, but seen on the scale of a whole structure this springback can lead to significant deviations in the geometry.

How can a grid be automatically generated on an arbitrary shape? – Several approaches have been discussed. They can be categorized in geometry, topology and structural. Geometrical approaches are based on principal curvature networks or other conjugate curve networks. However, with surfaces other than translational or rotational surfaces these curve networks seem unsuitable for meshing. Topological approaches initialize a coarse diagram which sets the main parameterization directions of the shape, after meshing and subdivision smooth grids can be generated. Concerning the generation of grids based on structural performance, initializing a grid based on the principal stress directions is mentioned, but just as with the conjugate curve networks mentioned earlier this might lead to unsuitable meshes, especially in relation to the geometrical approximation. Generating grids based on the topology of a shape provided the smoothest, simplest and most reliable grids by introducing singular vertices at the locations where a change in parameterization direction is necessary.

How can a double curved panel be rebuild into a developable surface and how to implement this for a shape formed by multiple panels? – Developable surfaces can be constructed by manually straightening one family of curvature lines. However, when dealing with multiple panels this leads to misalignments along the edges of the panels. Therefore this approximation should be approached as a global optimization problem. This global method modifies the shape as a whole in order to achieve developability in each panel. In order to do this, the entire shape is sampled with a certain amount of points, which are all forced towards local target planes.

What influence does the subdivision have on the developable surfaces and how does this affect the accuracy? – The biggest influence the subdivision has on the approximation results is the orientation of the grid edges. Grids based on principal curvature directions lead to better results with approximating the original shape by developable and even planar panels, according to the literature. However, as mentioned previously, subdivision based on principal curvature directions might lead to curve networks unsuitable for meshing when dealing with complex shapes.

9 Recommendations

Parts of the method that are proved to be working, such as the algorithm to construct a quad mesh based on the surface topology, could be used in practise to skip the manual steps of drawing grids on these kind of surfaces. However, currently the algorithm has some limitations such as rugged boundaries near high convex-and concave curvatures and large deviations in panel sizes, further research might provide methods to subdivide coarse meshes based on smoothness and panel size constraints.

This also applies to the structural analysis part, this could be a practical definition for a preliminary structural analysis. However, further research needs to be done in order to implement more realistic ways for analysing wind loads. The simplification to a projected load, colliding with the first panels it encounters, might not provide accurate results for complex shapes, in contrast to simple domes and cylindrical vaults.

The objectives in the shape approximation do increase the developability of the panels and are therefore proved to be working, however, full developability is not reached with the currently used objectives. Further research might lead to additional or different objectives in order to reach different results. Recommended research directions are already mentioned in Section 7.2.6, briefly summarized as:

- Instead of exerting higher forces on an entire neighbourhood of points related to a local target plane, future improvements could base this variation in strength on individual points rather than the local target planes.
- This method increases the developability locally, measured at each sample point. In order to increase the accuracy of the results, one might use a larger sample point size. This does however demand solutions for automatic face-sorting from the quad-tree order to a zigzag order.
- Approaching the global shape with developable stripes, where groups of panels share common target planes, could be an interesting topic for future research.

10 Reflection

10.1 Graduation process

Comparing this graduation topic with the different expertise in the Building Technology Chairs, it is best positioned in the Design Informatics Chair together with the Structural Design Chair. Mainly because of the amount of parametric modelling included in the research.

Up to this point there have not yet been mayor setbacks in the process, the approach and methodology did not change significantly. However, some parts of the methodology are stronger than others. The panelization based on the topological skeleton of a surface seems to be a good working solution to convert any surface topology into a quad mesh. And the theory from different research about this method gives it the scientific support. On the contrary, the redesign of the panels based on the Variational Shape Approximation methods found in the literature are not completely implemented in the algorithms yet. Significant time was spent on finding ways to indirectly modify surface normal vectors in order to align them with the desired plane. Despite the approach is not implemented flawlessly or on the scale of a complete shape, the approximation results of a single panel – as well as for a few panels – show that the objectives that are derived for the dynamic relaxation are correct and significantly increase the developability within a panel.

Research and design are very closely related in this project. Since the goal is to set up this parametric framework which has all sorts of different aspects included – such as quadrangular subdivision, mesh to NURBS conversion, shape approximation and structural analysis – research is done into these different aspects and results are implemented in the methodology and therefore as well in the design of the framework.

10.2 Societal impact

The result of this research is a framework partly implemented in a prototype design tool. Parts of the method that are proved to be working, such as the algorithm to construct a quad mesh based on the surface topology, could be used in practise to skip the manual steps of drawing grids on these kind of surfaces. This also applies to the structural analysis part, which could be a practical definition for a preliminary structural analysis. However, further research needs to be done in order to implement reliable ways for analysing wind loads. The objectives in the shape approximation significantly increase the developability of the panels and are therefore proved to be working, however, full developability is not reached with the currently used objectives. Further research might lead to additional or different objectives in order to reach different results.

In a way the approach followed by this framework contributes to a sustainable development. Currently steel loadbearing structures developed by AIP Partners, and possibly other companies as well, consist out of thick steel plates. Replacing these by sandwich panels to reach the same structural efficiency with less material, contributes to sustainable development in this sector. Besides this, the method to create the panels does not use the heavy machinery that is currently used in the curving of thick sheets.

References

Bailly, D., Bambach, M., Hirt, G., Pofahl, T., Della Puppa, G., & Trautz, M. (2015). Flexible Manufacturing of Double-Curved Sheet Metal Panels for the Realization of Self-Supporting Freeform Structures. *Key Engineering Materials*, *639*, 41–48. https://doi.org/10.4028/www.scientific.net/kem.639.41

Derks, J. P. B. N. (2012, October 6). De Eurocode sneeuwbelasting nader bekeken. *Roofs*. Retrieved from http://www.dakweb.nl/nl/roofs-2012-10-06-de-eurocode-sneeuwbelasting-nader-bekeken

Gavriil, K., Schiftner, A., & Pottmann, H. (2018). *Optimizing B-spline surfaces for developability and paneling architectural freeform surfaces*. Retrieved from https://www.researchgate.net/publication/327201813_Optimizing_B-spline_surfaces_for_developability_and_paneling_architectural_freeform_surfaces/related

Ghang, L., & Seonwoo, K. (2012). Case Study of Mass Customization of Double-Curved Metal Façade Panels Using a New Hybrid Sheet Metal Processing Technique. *Journal of Construction Engineering and Management*, *138*(11), 1322–1330. https://doi.org/10.1061/(asce)co.1943-7862.0000551

Grande, E., Imbimbo, M., & Tomei, V. (2018). Role of global buckling in the optimization process of grid shells: Design strategies. *Engineering Structures*, *156*, 260–270. https://doi.org/10.1016/j.engstruct.2017.11.049

Hoogenboom, P. C. J. (n.d.). Note on Stresses in Shells: Handout 8 [Presentation slides]. Retrieved May 9, 2019, from http://homepage.tudelft.nl/p3r3s/b17_schedule.html

Li, M. Z., Han, Q. G., Cai, Z. Y., Liu, C. G., & Su, S. Z. (2014). Multipoint Forming. *Comprehensive Materials Processing*, *3*, 107–147. https://doi.org/10.1016/B978-0-08-096532-1.00309-5

Liu, Y., Pottmann, H., Wallner, J., Yang, Y., & Wang, W. (2006). Geometric modeling with conical meshes and developable surfaces. *ACM Transactions on Graphics*, *25*(3), 681. https://doi.org/10.1145/1141911.1141941

McCormick School of Engineering and Applied Science, Northwestern University. (n.d.). Incremental Forming at Multi-scales. Retrieved January 7, 2019, from http://ampl.mech.northwestern.edu/research/current-research/incremental-forming-macro.html

Mesnil, R., Douthe, C., & Baverel, O. (2017). Non-Standard Patterns for Gridshell Structures: Fabrication and Structural Optimization. *Journal of the International Association for Shell and Spatial Structures*, *58*(4), 277–286. https://doi.org/10.20898/j.iass.2017.194.893

Mesnil, R., Douthe, C., Baverel, O., & Léger, B. (2017a). Linear buckling of quadrangular and kagome gridshells: A comparative assessment. *Engineering Structures*, *132*, 337–348. https://doi.org/10.1016/j.engstruct.2016.11.039

Mesnil, R., Douthe, C., Baverel, O., & Léger, B. (2017b). Generalised cyclidic nets for shape modelling in architecture. *International Journal of Architectural Computing*, *15*(2), 148–168. https://doi.org/10.1177/1478077117714917

Oval, R., Rippmann, M., Mesnil, R., Van Mele, T., Baverel, O., & Block, P. (2018). *Topology Finding of Structural Patterns*. Paper presented at Advances in Architectural Geometry 2018, Gothenburg, Sweden. Retrieved from http://thinkshell.fr/library/structural-patterns-masonry-vault-design-r-oval-et-al-2018/

Pellis, D., & Pottmann, H. (2018). Aligning principal stress and curvature directions. In L. Hesselgren, A. Kilian, S. Malek, K. G. Olsson, O. Sorkine-Hornung, & C. Williams (Eds.), *Advances in Architectural Geometry 2018* (1st ed., pp. 34–53). Retrieved from https://research.chalmers.se/publication/504188/file/504188_Fulltext.pdf

Pottmann, H., Eigensatz, M., Vaxman, A., & Wallner, J. (2015). Architectural Geometry. *Journal Computers and Graphics*, *47*(C), 145–164. https://doi.org/10.1016/j.cag.2014.11.002

Preisinger, C. (2018). *Karamba3D Parametric Engineering: User Manual* (Version 1.3.1). Retrieved from https://www.karamba3d.com/download/#manual

Rigby, D. (2003). TopMaker: A Technique for Automatic Multi-Block Topology Generation Using the Medial Axis. In *ASME/JSME 2003 4th Joint Fluids Summer Engineering Conference* (pp. 1991–1997). Honolulu, Hawaii, USA. https://doi.org/10.1115/FEDSM2003-45527

Sechelmann, S., Rörig, T., & Bobenko, A. I. (2013). Quasiisothermic Mesh Layout. In L. Hesselgren, S. Sharma, J. Wallner, N. Baldassini, P. Bompas, & J. Raynaud (Eds.), *Advances in Architectural Geometry 2012* (pp. 243–258). Wien, Austria: SpringerWienNewYork.

Tam, T. K. H., & Armstrong, C. G. (1991). 2D finite element mesh generation by medial axis subdivision. *Advances in Engineering Software and Workstations*, *13*(5–6), 313–324. https://doi.org/10.1016/0961-3552(91)90035-3

Tang, C., Bo, P., Wallner, J., & Pottmann, H. (2016). Interactive Design of Developable Surfaces. *ACM Transactions on Graphics*, *35*(2), 1–12. https://doi.org/10.1145/2832906

Winslow, P., Pellegrino, S., & Sharma, S. B. (2008). Mapping Two-Way Grids Onto Free-Form Surfaces. *Journal of the International Association for Shell and Spatial Structures,*, *49*(2), 123–130. Retrieved from http://www-civ.eng.cam.ac.uk/dsl/publications/Mapping_two-way_grids.pdf

Winslow, P., Pellegrino, S., & Sharma, S. B. (2009). Multi-objective optimization of free-form grid structures. *Structural and Multidisciplinary Optimization*, *40*(1-6), 257–269. https://doi.org/10.1007/s00158-009-0358-4

Zuo, Q., He, K., Dang, X., Feng, W., & Du, R. (2017). A Novel Incremental Sheet Bending Process of Complex Curved Steel Plate. *Journal of Manufacturing Science and Engineering*, *139*(11), 1–12. https://doi.org/10.1115/1.4037428

Appendix

A: Approximation of free-form geometry (Literature study)

Defining the objective

Concerning the process of designing free-form shapes, there are two main terms of importance. *Panelization* and *rationalization,* in the literature also called *segmentation* and *approximation* respectively. (Pottmann et. al, 2014) The first being the process of dividing the surface of the geometry into small(er) producible panels, and the latter being economically optimizing sizes and shapes of the panels. The process of maximizing approximation quality is called *Variational Shape Approximation.* (Ghang & Seonwoo, 2012; Pottmann et. al 2014) Rationalizing can be done in different ways, but is really dependent on the production methods used. If mainly moulds or dies are used, the main objective would be to minimize the amount of unique panels, in order to reuse a die as much as possible.

In what proportions panelization and rationalization are necessary depend on the used design strategy. Mesnil et al. (2017) describe multiple design strategies , using the term morphogenesis:

- *Geometrically-constrained morphogenesis* focusses on shapes with properties that simplify their fabrication such as working with surfaces of revolution, developable surfaces or planar surfaces. The feasibility of the design based on the materialisation and costs for production of the design shape. For instance a shape could be form-found using a (number of) standardised elements.
- *Mechanical-constrained morphogenesis* is related to shaping surfaces with good mechanical properties. These shapes are usually the result of form-finding processes.
- *Flexible morphogenesis* is related to other aspects such as comfort, ornamentation and overall aesthetics. Since this design strategy does not take into account structural behaviour and constructability, a post-rationalization in necessary to make sure the structural- and fabrication requirements are met.

The first two methods might limit the design freedom, while the last method may need a lot of post rationalisation. Other approximations are done with polyhedral surfaces, developable surfaces and double-curved surfaces. Each having their own pros and cons according to their definition as described in Pottmann et. al (2014):

- *Polyhedral surfaces* consist out of planar panels. Different patterns in panelization are possible such as triangular meshes, quad meshes, hexagonal meshes and so on.
    - *Triangular meshes* are easiest to work with since the vertices are able to move during designing, while remaining it's planar faces. In general constructions with triangular panels are more complex to assemble due to their valence 6 vertices (each vertex connected to 6 edges).
    - *Quad meshes* are more difficult to represent a negatively (Gaussian) curved surface, unless the mesh is based on very sharp cornered quads. An advantage of nearly rectangular quad panels is the fact that these shapes lead to less waste material since the base plates where the panels are cut out of are also rectangular. The best way to create nearly rectangular panels when approximating a surface is by following the principle curvature lines of the surface in the meshing. Isothermic surfaces are easiest to divide in quads with fixed aspect ratio, these are surfaces of rotation, surfaces of

constant mean curvature and minimal surfaces. Surfaces following from physical form-finding methods are close to isothermic surfaces as well. (Sechelmann et al., 2013) This however, may restrict the design freedom.

    - *Hexagonal meshes* are more complicated to design, due to the valence 3 vertices non-convex shapes could arise. A method for creating these meshes could be to start with a triangular mesh and use the dual representation to convert it to a hexagonal mesh.
- *Developable surfaces* are single-curved surfaces which can be unfolded into a 2D plane without stretching or tearing. Such a surface could be created using developable strips or geodesic strips, the latter being straight strips following geodesic curves. Developable surfaces can be based on cones and cylinders and consist out of a ruled surface with the additional property that the tangent plane along a ruling is constant. (Tang et al, 2016) This is an important condition developable surfaces must meet.
- *Double-curved surfaces* are the most accurate way of representing a free-form surface. However, in order to economically justify these surfaces a rationalization is still required. Ruled surfaces are the most promising type of geometry to efficiently produce. Repetition also increases the manufacturing efficiency, including this in the design could lead to the use of a rotational symmetry or basing the shape on a sphere or torus. However, this is the case if moulds are used in the process. In the next section production methods are discussed.

When modelling with curved surfaces there are 3 mayor continuity conditions as described by Li et. al (2014). (Figure 29) The first being location continuity (G^1), then tangent continuity (C^1) and lastly curvature continuity (G^2). For the purpose of approximating doubly-curved surfaces, we aim for G^2 continuity, which can be expressed as followed. Two joint NURBS surfaces first need to have a common edge, so they must have location continuity (G^1). Additionally, the tangent of the edge curve and the tangents of both surfaces in a vertex along the edge must be coplanar.

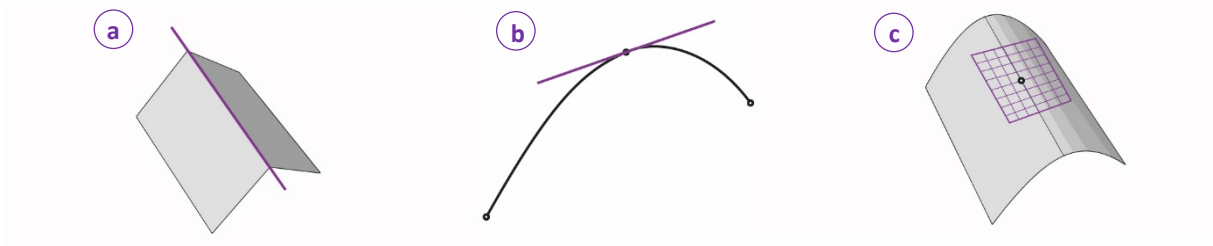

Figure 29: The three mayor types of continuity conditions: location continuity G^1 (a), tangent continuity C^1 (b) and curvature continuity G^2 (c).

Optimizing the panelization is not the main objective in architectural designs, since the seams are most of the time visible and therefore the panelization will mostly be based on aesthetics and the architect will have a mayor influence on this panelization. The main challenge would therefore be the rationalization. This means approximating the surface, with only small deviations from the existing subdivision of panels. However, patterns can arise in many forms such as different (functional) layers or just textures and penetrations. (Pottmann et. al, 2014)

Developable surfaces

As mentioned before, developable surfaces can be unrolled without stretching or tearing. Besides this they can approximate geometry more accurate than planar surfaces because of their curved nature, without the disadvantages that double-curved surfaces bring with them. These are discussed in the next section. Basically a developable surface consists out of an envelope of multiple planes. All planes intersect the surface along a straight line, which together form the rulings of the surface. (Liu et al., 2006) The authors distinguish three types of rulings. First of all, the parallel rulings which create

cylinder surfaces. Secondly, rulings that pass through a fixed point, creating a conical surface. Finally, rulings that are tangent lines of a singular space curve, this will form a tangent surface.

According to Tang et al. (2016) today's CAD systems still present difficulties with developable surfaces. The *lofting* principle, which defines a developable by its boundary, comes close but does not yet work flawless in every situation. A reason for this is the nonlinear nature of developability, these surfaces do not only consist out of ruled surfaces but also have the property that the tangent plane along a ruling is constant. The authors describe a computational setup where all edges of a mesh are labelled and therefore each panel can be identified according to a certain surface type based on its adjacent edges. The edges are either labelled as a ruling (***R***) or as a spline (***S***), with the first representing a straight line and the latter representing a curve. Different types can be distinguished as following: (Figure 30)

- ***S R S R*** = Corresponds to a spline developable.
- ***S R S*** = Corresponds to a spline developable degenerating into a point.
- ***S R R*** = Corresponds to a spline developable, but the spline boundary is degenerating into a point. In other words this is a conical surface.
- ***R R .. R*** = Corresponds to a planar polygon.

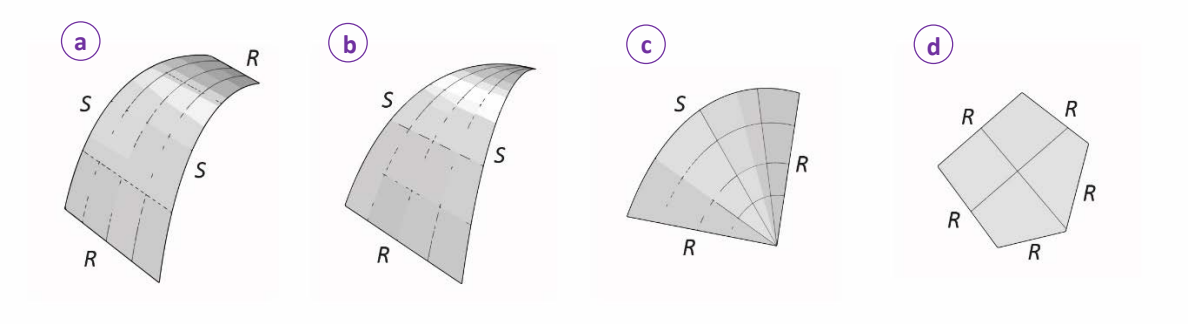

Figure 30: Different types of mesh faces: SRSR, SRS, SRR and RRRRR.

The authors emphasize the importance of a combinatorial consistency. To each vertex of the mesh a location is assigned and to each (spline) edge an orientation with a certain control point sequence. For an ***S R S R –*** surface the corresponding spline edges are e_0 and $-e_2$. What may seem obvious, but what is a requirement for the alignment of panels, is that for any (spline) edge in face f_1 and f_2 the curves $c_{e,f1}$ and $c_{e,f2}$ must be the same geometrically. Therefore the degree, smoothness and parameter intervals must be the same. For two surfaces sharing a ruling, the unit normal vectors of the tangent planes along the ruling should be equal for a perfect smoothness.

Increasing developability

Gavriil, Schiftner & Pottmann (2018) propose a method to increase the developability based on the Gauss image of the surface. A side note should be that their method focusses on *almost* developable surfaces, as they assume most materials allow for a bit of stretching during assembly and still make use of the cheaper production for developable surfaces. They separate three different geometries based on their Gaussian curvature:

- *Constant zero Gaussian curvature* surfaces are developable surfaces and the geometry of the surface is Euclidean geometry.
- *Positive Gaussian curvature* surfaces are spherical surfaces and the geometry of the surface is a Spherical geometry.
- *Negative Gaussian curvature surfaces* are pseudo-spherical surfaces and the geometry of the surface is a Hyperbolic geometry.

The developability is increased using an algorithm that flattens the Gauss image locally. Another method would be to shorten one family of principle curvature lines, in this way they will become (almost) straight and the surface will therefore become developable. If we go back to the method described by Gavriil, Schiftner & Pottmann (2018), it can summarized in the following steps: (Figure 31)

- A surface S^2 is divided in *u* and *v* parameters. This surface is sampled at several points based on the *u-, v*-parameters, these are the sample points p_k.
- The panels consist out of a group of sample points p_k. In order to protect the continuity of the surface, bigger patches are used which have at least 1 overlapping row of sample points at each side. In the paper referred to as patches N_j, are therefore represented by a bigger group of sample points p_k.
- A target plane, referred to as H_j, is initialized passing through the barycentre of N_j with a unit normal as orthogonal as possible to the set Q_j of main principle directions.
    - A weight factor w_k is also introduced, a low weight factor indicates the difficulty in distinguishing between the two principal curvatures. This factor corresponds to each sample point p_k and is used for initializing plane H_j. This plane will be the target plane for all normal vectors n_k of p_k.

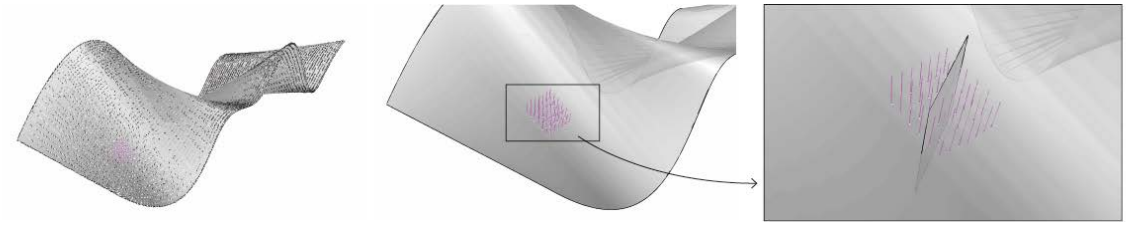

Figure 31: Visualization of the sample points (p_k) on the surface (left), the surface normals (n_k) at the sample points in a patch (middle) and the initialized target plane (H_j) in the direction of the maximum principal curvature (right).

For the optimization process is not one solution, therefore different terms with different weights are added to guide towards a solution. (Tang et al., 2016) In order to do this and flatten the Gauss image of the surface – and therefore increase the developability – different energy terms are constructed. In this way they is an numerical value to minimize in the optimization process. (Gavriil, Schiftner & Pottmann, 2018) The energy terms that the authors use are:

- Developability Energy $\boldsymbol{E_d}$ takes into account the sum of distances of the normals n_k on the surface to the target patch plane H_j.
- Closeness Energy $\boldsymbol{E_c}$ measures the closeness of the resulting surface *S* to a reference surface S_{ref}, which would be the initial design surface.
- Final Fairness Energy $\boldsymbol{E_f}$ is introduced to provide a smoothening effect. Is consists of the sum of first and second order differences of the control points in both grid directions.
- Rotationality energy $\boldsymbol{E_r}$ is introduced to include the possibility for rotational surfaces such as rotational cones or rotational cylinders. These surfaces have the property that the surface normal lines are coplanar with the axis of rotation.
- All energy forms are assigned their own weights w_d, w_r, w_c, and w_f and therefore the total energy is defined as:

$$E = w_d E_d + w_r E_r + w_c E_c + w_f E_f \quad (1)$$

The theory of Gavriil, Schiftner & Pottman (2018) as described above narrows the assignment down to the minimization of the total energy, with variables w_d, w_r, w_c, and w_f. Different ratios of these values will lead to different outcomes, depending on the wishes of the designer.

Optimizing for developability

The method of Gavriil, Schiftner & Pottmann (2018) as described in the previous paragraph, is a method for Variational Shape Approximation to get developable segments (panels) to represent the whole shape. Other methods of Variational Shape Approximation described in literature such as from Liu et al. (2006) are very similar, even if their goal is to realize planar panels instead of developable panels. In principle the methods create an 'energy term' which is described by a Langrangian function. This Langrangian function combines multiple constraints in order to have one value to minimize by changing the variables in the geometry. The main differences lay in the definition of the constraints and which constraints are used. The latter of the methods mentioned above has an additional angle constraint to prevent intersecting edges and therefore singular curves. (Liu et al., 2006) This angle constraint forces the sum of all angles in a quad panel towards 2π. Oval et al. (2018) introduces a new term to the equation related to the skewness of a panel. This term tries to prevent sharp corners in a panel, on the one hand to prevent complex connections and on the other hand to reduce waste from cutting the panels. The more rectangular the shapes are, the less waste material will arise during the cutting process. (Oval et al., 2018)

However, these methods change the shape as a whole in order to come as close as possible to developability per panel, while preserving the smoothness of the final shape and closeness to the original shape. In which proportions each target is reached is determined by weight factors corresponding to the desire for either a full developable surface, a high accuracy to the original surface, a smooth surface, or somewhere in between all of these goals.

A logical consequence of this method is a deviation from the original surface when the goal is to reach absolute developability. This has to do with the fact that these methods, for each panel, take into account all the adjacent panels to preserve the smoothness of the end result. According to Liu et al. (2006) higher accuracy to the original surface can be reached if the panelization is derived from principal curves or other conjugate curve networks.

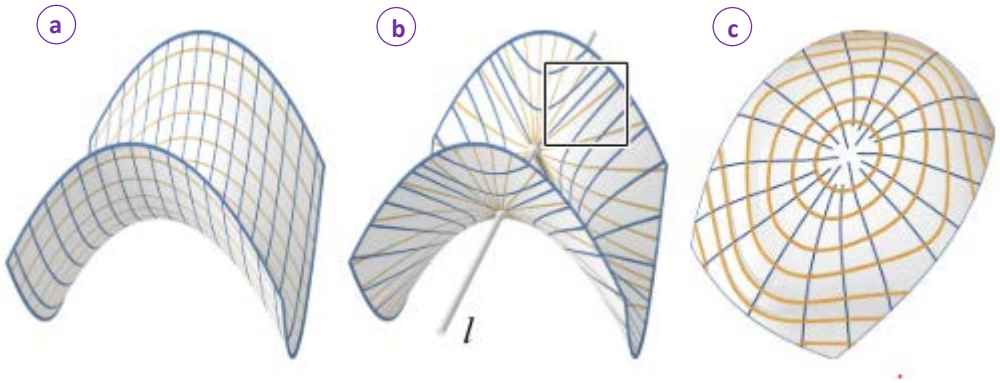

Figure 32: Different types of conjugate curve networks. (Liu et al., 2006, p. 683)

A. In a translational surface the (u,v)-parameter curves are conjugate. A surface is a translational surface if its created by translation of a curve along another curve. (Figure 32a)
B. For all surfaces, the intersection curves of planes through a fixed line (Figure 32b, yellow curves) and the contour generators (Figure 32b, blue curves).
C. The isophotes (Figure 32c, yellow curves) and the curves of steepest descent (Figure 32c, blue curves). To clarify, an isophote has the property that the surface normal along the curve forms a constant angle with the Z-axis. In computer graphics an isophote can also be described as a curve through points of equal brightness on an illuminated surface, in general these curves are used to check whether surfaces or panels align smoothly. No kinks in the curves means the surfaces have G^2 continuity. (see section 6.1.1)

According to Pellis and Pottmann (2018) designing freeform architectural surfaces in regard to economic and feasibility requirements is challenging on its own, but rationalizing such surfaces by means of quadrilateral meshes following principal curvature lines is beneficial for manufacturing reasons, such as the possibility for developable panels while preserving the closeness to the original shape and simplified substructure connections. Having the panelization based on for example the principal curvatures, could also prevent high skewness in the panels. (Oval et al., 2018) “Principal meshes are discrete versions of principal curvature parameterizations of surfaces.“ (Pellis & Pottmann, 2018, p.35) However, these principal meshes and conjugate curve networks described above are not always suitable for panelization. This can already be seen in the results of Figure 32. The suitability of a curve network is dependent on the type of surface one is dealing with. Only type A could be suitable as long as the design surface is a translational surface, and type C as long as there is no change from convex to concave curvature. The same rule goes for principal curvature lines, as long as the curves do not intersect transversely the curve network is not suitable for panelization and meshing.

B: Generating a quad grid on a surface (Literature study)

Meshing based on surface topology

Designing an efficient quad grid on a complex (curved) surface is a challenge on its own, especially when the design is intended for structural purposes such as self-supporting pavilions or roof structures. The design of a grid is influenced by different factors such as aesthetics, structural performance, fabrication, assembly, sustainability and costs. (Oval et al., 2018) These surfaces will most likely perform as (grid)shell structures. Shell structures can span large areas efficiently due to their double curvature that provides geometrical stiffness. These structures are often expressed in a pattern, which resembles the load-bearing system once the structure is assembled.

Rigby (2003) describes a method for topology generation based on the medial axis. (Figure 33) He states that a major part of the time required for the generation of a grid is spent on the designing of the topology. With methods to initialize a coarse quad mesh topology based on the medial axis this process can be shortened. The method he describes works for general configurations, these are defined as a collection of non-intersecting two-dimensional closed curves. In this process irregular nodes arise, which are defined as points where more than four quads meet. These topological singularities are necessary for dividing the shape into simpler quadrangular regions. (Rigby, 2003) The singularities are derived from the earlier mentioned Medial Axis of the object, introduced by Blum (1967). The research of Tam and Armstrong (1991) present a two-phased method for mesh generation. The first phase is the subdivision where the Medial Axis is used to divide these complex shape configurations into simpler regions which are further broken down into quads suitable for meshing.

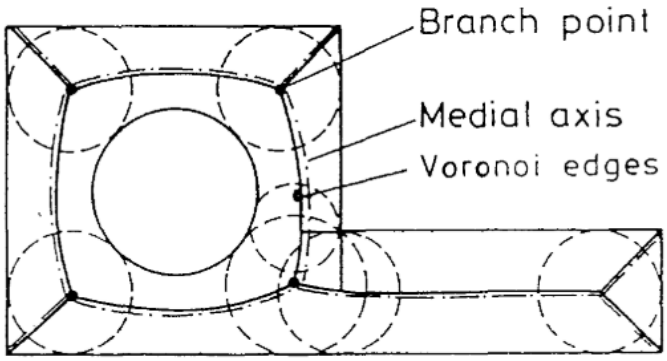

Figure 33: Vonoroi diagram and medial axis of a 2D object. (Tam & Armstrong, 1991, p. 314)

The Medial Axis is constructed by interpolating a collection of points, which all have an equal distance to at least two points on the boundary curves. (Rigby, 2003) Figure 33 shows an example of the Medial Axis, as well as the Voronoi edges of a shape. It can be seen that the Medial axis branches out at certain points, these branch points are defined as the topological singularities as described earlier. Tam and Armstrong (1991) state that there exist different methods for deriving the Medial Axis, but the most general and reliable approach is based on the Delaunay triangulation of points distributed along the shape boundaries with a high density. Figure 33 also shows that the Medial Axis aligns with the Voronoi edges in the shape. However, extracting the desired edges from the complete Vonoroi diagram is difficult and besides this modifications need to be made to the Medial Axis to reach the final quadrangular divisions for the coarse quad mesh. Since the Vonoroi diagram is the dual representation of a Delaunay triangulation, a Delaunay meshing of the points along the boundary curves provides an useful basis for retrieving the Medial Axis. In this Delaunay mesh important information about singularities and adjacencies is stored. The Medial Axis is then constructed by interpolating the center

points of the circumcircles of the vertices of each Delaunay triangle, the smaller the distance between the points on the shape boundary, the more accurate this Medial axis will be. (Tam & Armstrong, 1991)

The authors mentioned above, use the underlying Delaunay triangulation to identify different points based on different triangles for making modifications to the Medial Axis. Different types of triangles identified by Tam and Armstrong are: (1991)

- *Junction type (J)* triangles touch the geometry at three different entities, without one of the edges laying on the object boundary. This means these triangles have 3 adjacent faces to it and therefore the circumcentre is at a branch point on the Medial Axis where three branches meet.
- *Intermediate type (I)* triangles also touch the geometry at three different entities. However, they have one of the triangle edges positioned on the object boundary and is also connected to a concave vertex of the object.
- *Corner type (C)* triangles as well touch the geometry at three different entities. One of which is a convex vertex of the object and the two adjacent edges of this vertex are on the object boundary. This means that this triangle type only has one adjacent face and therefore its circumcentre forms an end point of the Medial Axis.
- *Topologically redundant type (T)* triangles can occur at places in the object where the edge geometry is curved. All three vertices are on the same arc and therefore its circumcentre is located at the arc centre of curvature. These triangles correspond to an endpoint of the Medial Axis as well.
- *Normal Type (N)* triangles correspond to triangles that touch two different entities with none of them being a vertex of the object boundary. Additionally one of the edges is located on the object boundary. This is the most occurring triangle type, as they contain the circumcentres connecting the branch- and end points of the Medial Axis. For simplification in Figure 34 they are combined into larger triangles.

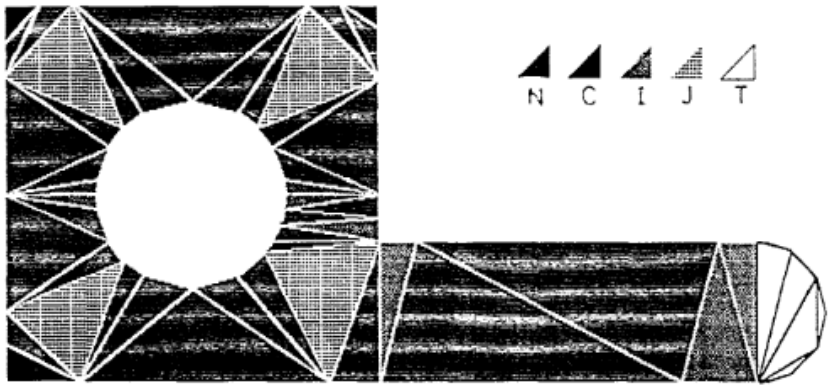

Figure 34: Different types of triangles within the Delaunay triangulation as decribed by Tam & Armstrong (1991, p.315)

Based on these defined types of triangles in the Delaunay triangulation different type of points can be identified according to Rigby: (2003)

- *Normal vertex (N)* which has at least three touch points that define it, each normal vertex has three locations on the boundary curves that have an equal distance to it. These also form the singular vertices in the shape. This vertex is the circumcentre of a *junction type* triangle.
- *Corner vertex (C)* which occurs at a concave discontinuity on the boundary. This is the vertex of a *corner type* triangle located at a concave discontinuity on the boundary.
- *Dangle vertex (D)* which occurs where the boundary passes through a maximum in convex curvature. This vertex is the circumcentre of a *topologically redundant type* triangle.

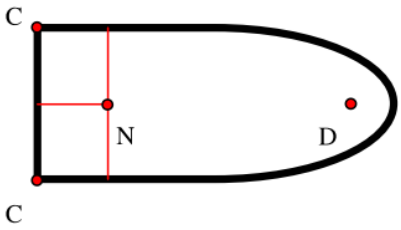

Figure 35: Different types of vertices described in the research of Rigby (2009, p. 2)

The circumcentres of the *intermediate type* and *normal type* of triangles is only used for interpolating the edge curves through. Each connection between different pairs of vertices is identified as a different edge type. The exact physical shape of the medial edges is not necessary to retrieve the connectivity between the different vertices however. (Rigby, 2003)

Once the above described vertices of the Medial Axis are found, the object can be reduced to a collection of simpler meshable regions. (Tam & Armstrong, 1991) However, the authors propose additional modifications to convert non-quadrangular regions to quadrangular regions. Figure 36 visualizes how the authors modify non-quadrangular regions.

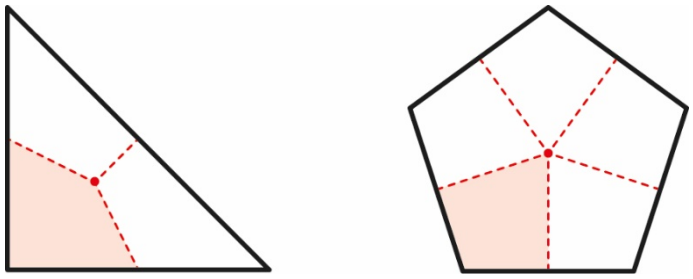

Figure 36: Modification necessary to convert 3-sided regions (a) and 5-sided regions (b) to quadrangular regions.

In the previously discussed research the authors clearly define the vertices and connections necessary to construct the Medial Axis, but Oval et al. (2018) describe a more general method for initializing a coarse quad grid based on this Medial Axis, using the same principles of the previous discussed research. This coarse quad grid defines the parameterisation directions of the shape. A subdivision can be applied afterwards to set the desired density based on either aesthetic, structural or fabrication requirements. The coarse quad grid is based on this topological skeleton following the steps described by Oval et al. (2018):

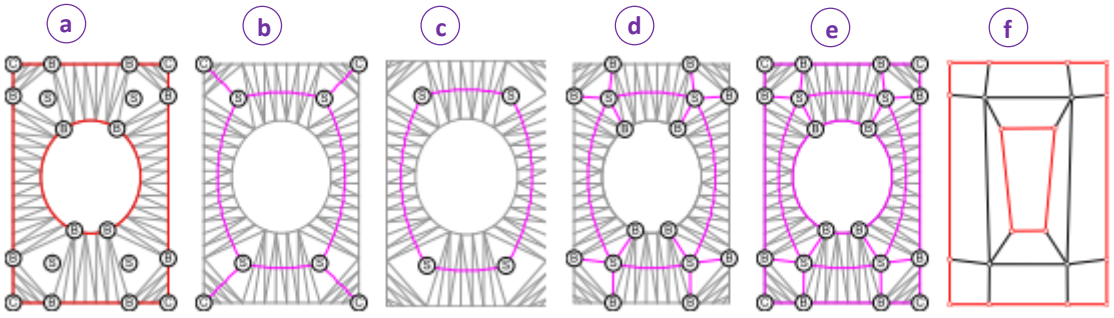

Figure 37: Different steps for initializing a coarse quad mesh based on the topological skeleton of the surface. (Oval et al., 2018, p. 5)

A. The input surface of the object is mapped to a plane and all boundaries are divided into a set of vertices for a Delaunay triangulation and meshing. This mesh consists mainly out of valence 2 faces, which means a face is adjacent to two other faces. Besides these, some valence 3 faces arise, which are the singular faces in the mesh. These singular faces form an important

element in this method. After this Delaunay triangulation different key points can be identified. First of all the circumcentres *S* of the singular faces, secondly all boundary vertices *B* of the singular faces, thirdly the corners *C* of the shape boundaries and finally all the circumcentres of the other faces. The corners *C* can be recognised as valence 2 vertices.

B. The medial axis (Blum, 1967) is initialized by connecting the *S* vertices with the *C* vertices via the circumcentres of adjacent faces as well as connecting all *S* vertices with each other, also via the circumcentres of all adjacent faces. The medial axis therefore exists out of S-C branches and S-S branches.
C. To generate a course quad mesh, some modifications need to be made, starting with pruning the S-C branches from the medial axis.
D. The next step is to create the connection between the point *S* and points *B* for each singular face, to graft the S-B branches.
E. Together with all boundary curves, the S-S branches and S-B branches form a scheme that represents the connectivity of the coarse mesh.
F. The last step is to generate a coarse mesh based on the constructed connectivity between the vertices.

In this method the complexity is reduced to the use of a system where there are only singular faces, normal faces and corner faces. The vertices used for the construction of the Medial Axis are the corner points (C) from corner faces, the circumcentres of the singular faces (S), and the circumcentres of the normal faces to interpolate a curve through when constructing the main branches. Next to this the boundary vertices (B) of the singular faces form important nodes which have not been introduced in the methods of Rigby (2003) and Tam and Armstrong (1991). Their work resulted in similar regions, but with more complex methods.

The resulting coarse mesh can be a basis for optimizations related to structure or other purposes, as mentioned before this coarse mesh provides the parameterization directions of the shape. From this point on subdivision methods, for example the Catmull-Clark subdivision method, can be used to densify the coarse mesh. Afterwards this mesh can be relaxed on the object surface to increase the accuracy of the mesh towards the original surface. As addition to this method, it could be interesting for roof-type structures to manually or parametrically input singular points at the location of columns. As described by Oval et al. (2018), including these points in the Delaunay triangulation will introduce singular points in the mesh, where locally all edges will be converged into that point. Besides to structural reasons, adding singular points could also be desired at umbilical points in the geometry.

Optimizing grids for structural performance

The term ‘grid shell’ refers to structures with the strength and shape of a curved shell, but consist out of a grid of beams instead of solid surface. (Grande, Imbimbo & Tomei, 2018) According to their research, structural optimizations can consist out of *shape optimization, size optimization* and *topology optimization*. Usually the shape is designed by an architect and cannot change significantly, but the topology of a grid and the sizing of the rods are parameters that can still be adjusted based on certain objectives. The objectives can be related to serviceability and utilization criteria such as displacements, stiffness, stress and buckling loads, but as well to minimizing the total weight or material volume. (Grande, Imbimbo & Tomei, 2018)

Existing tools make use of relatively simple geometrical rules and algorithms to map a grid onto a surface. (Winslow, Pellegrino & Sharma, 2008) However, this does not relate to any fabrication or structural performance constraints. In their research the authors emphasize that important objectives for the structural analysis and optimization for (grid)shell structures are not only utilization and serviceability criteria, but global buckling criteria as well. By including a buckling analysis in the design stage rather than as a verification in the end, the design of the grid could be adjusted based on these

criteria, rather than just increasing the cross-sections in the grid. (Grande, Imbimbo & Tomei, 2018; Winslow, Pellegrino & Sharma, 2008)

In their research Winslow, Pellegrino & Sharma (2008) divide a surface into different regions based on the curvature of the surface and the grid direction is set individually for each region. Figure 38 shows that the vertices in the grid are shifted in order for the grid to align as much to the principal stress directions as possible. To do this the surface is meshed with shell elements and at the centroid of each element the principal stress directions are computed. (Winslow, Pellegrino & Sharma, 2009)

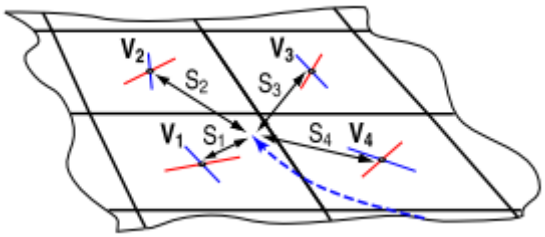

Figure 38: Scheme of grid initializing based on principal stress directions. (Winslow, Pellegrino and Sharma, 2008, p. 6)

In further research Winslow, Pellegrino & Sharma (2009) took it further and wrote a Multi-Objective Genetic Algorithm to vary grid directions per region of the surface. However, the downside of these structural optimizations is that the outcome of these optimizations is the optimum solution for a single load case. (Figure 39) When the loading conditions change, different orientations are necessary to create the new optimum solution. Of course, a combination of the most occurring load cases could provide a good input for an optimization, as long as other load cases are considered in the verification of the structure.

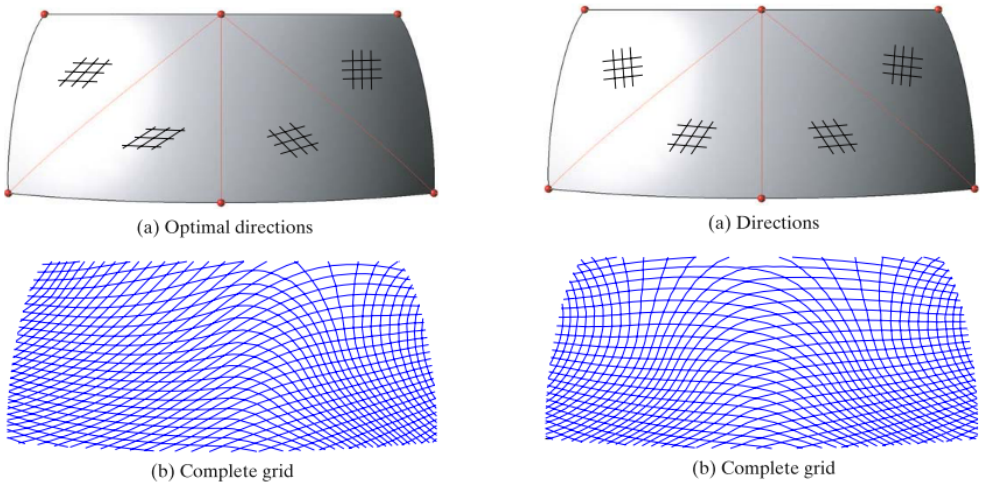

Figure 39: Optimal grid directions based on different loadcases. (Winslow, Pellegrino & Sharma, 2009, p. 267-268)

Non-standard patterns in grid shells

Before quad grids were discussed together with methods to improve their structural performance by adjusting the grid orientation. The reason for this is the fact that this grid must be the underlying load-bearing structure for the quadrangular steel sheets that form the architectural expression of the structure. However, this underlying grid could still differ from the finishing panels. In the literature different non-standard patterns are compared with other (non-)standard patterns based on their structural performance. An important factor is the existence of torsion-free nodes in the structure. Ideally the node axis of a torsion-free beam layout should be normal to the surface to generate torsion-

free nodes. (Mesnil et al., 2017a) Quad grids seemed to make a good solution for this, but there are other patterns with a node valence of 4 as well. (Mesnil, Douthe & Baverel, 2017)

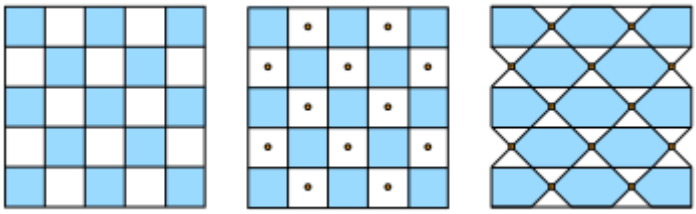

Figure 40: Quadrilateral grid vs kagome grid. This image shows the steps necessary to convert a quad grid to a kagome grid. (Mesnil et al., 2017b, p. 343)

An example of another grid with a node valence of 4 is the kagome-grid. In their research Mesnil, Douthe & Baverel (2017) state that planar kagome (PK) grid shells outperform planar quadrilateral (PQ) grid shells. According to their research and case studies they found that the optimal PQ grid shells have 60% more beams or connection details than PK grid shells. However, their research neglected material, geometry and connection imperfections. Working with consistent materials and CNC machines could reduce these imperfections.

When comparing quadrilateral grids with kagome grids, the quadrilateral grids rely mostly on the bending stiffness of the node connections, whereas the kagome – as well as other triangulated – grid shells benefit from a shell like behaviour without the need for rigid connections. (Mesnil et al., 2017b) Because kagome grids have a node valence of 4 like quadrilateral grids, instead of 6 for triangular grids, the nodes are less complex while they still benefit from the geometrical stiffness delivered by the triangulated cells just as in a regular triangular grid. This could be explained by the fact that there are beam elements in multiple directions, which means there will be more axial forces in the structure instead of bending moments in the beams.

The authors do state that these grid shells are not compared to other solutions such as cable-braced or triangular grid shells which might be structurally more efficient since these cable stiffeners are very lightweight. However, an important argument against this is that steel contractors might prefer to build moment connections rather than installing cables. (Mesnil et al., 2017b)

C: Production methods (Literature study)

The process of rationalization that is mentioned in the previous section is of main importance for architectural applications, since most panels will be unique. Mass-production technology's for double-curved shapes exist, but often make use of expensive moulds that will require a lot production time, costs and in the end waste material. Because of the requirement for unique panel shapes these methods are not feasible. (Ghang & Seonwoo, 2012) Double-curved steel plates have been widely used in the ship industry, but the production methods used are still deeply dependent on the manual operation of skilled workers. (Zuo et. al, 2017) In this section several production methods are discussed ranging from conventional methods to new innovative adjustments to them.

Multipoint forming and variations

There are of course other methods for bending sheet metal, of which a few are discussed by Ghang & Seonwoo (2012) each with its advantages and disadvantages for a specific case study project. However, general pros and cons of each method do become more clear. Multipoint forming seems to be an appropriate method of bending sheet metal, and this has been applied in for instance the production of the "Bird's nest" façade in the Beijing National Stadion. (Li et al., 2014) Ghang & Seonwoo (2012) present three variations on multipoint forming:

- *Multipoint Forming* with a rubber mat between the work piece and the computer controlled pins. (Figure 41a) The machine consists out of an upper and lower die with each a grid of computer controlled pins that are adjustable in height. Therefore this method provides a huge advantage compared to traditional die forming, since the dies can adapt and therefore do not produce any waste material, production time and storage space. (Li et. al, 2014) The main disadvantage this method has that it may create small punches in the final surface due to the more concentrated point loads from each pin. However, when using a rubber – or another flexible material – in between the work piece and the pins, this can be reduced or even avoided.
- *Multi-post Hydroforming*, a combination of multipoint forming and hydroforming. (Figure 41b) The lower die of the multipoint forming method is used, but hydraulic pressure is used to press the work piece in the desired shape. However, in the tests of Ghang & Seonwoo (2012) the pressure turned out to be too strong and leave dents on the surface, even when a rubber mat was applied on the pins.
- *Multipoint Stretch Forming*, which is a combination of multipoint forming and stretch forming. (Figure 41c) A lower die of the multipoint forming is used, and the blank sheets are stretched over the die using two-way stretch forming. This method is very useful for single-curved and slightly double curved shapes, but complex shapes might need to be pressed extra with the upper multipoint forming die. This is especially the case for panels with a hyperbolic geometry.

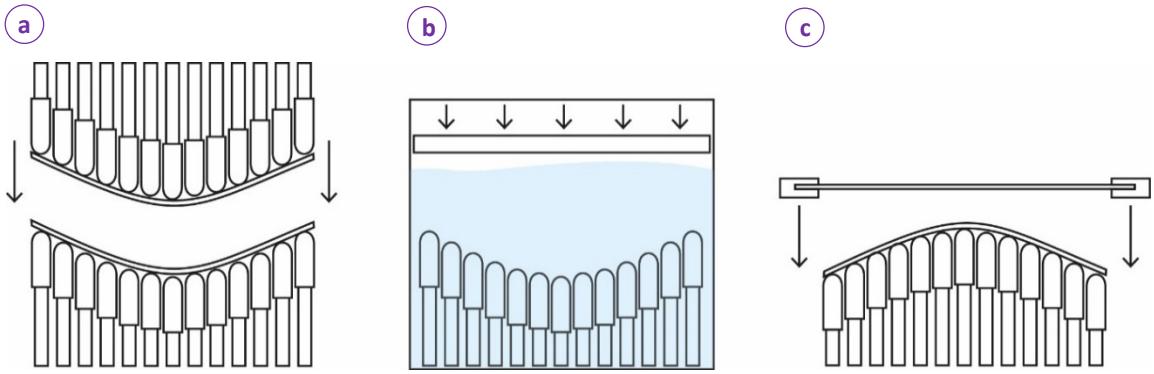

Figure 41: Three types of multipoint forming: Multipoint Die Forming, Multi-post Hydroforming and Multipoint Stretch Forming

An advantage of the first variant of Multipoint Forming, which can be seen as the regular Multipoint Forming, is that this method can also be used for larger plates – e.g. plates larger than the press. The plate would then be formed in steps, section per section with overlapping regions. However, with the regular Multipoint Die Forming the quality and accuracy is not guaranteed due to the uncontrollable distortion in the work piece. (Zuo et al., 2017) Due to the non-uniform distribution of forces the work piece might tear or wrinkle.

Li et al. (2014) present another adjustment to the multipoint forming method. They propose to use blank holders around the multipoint forming dies, in order to prevent the work piece from wrinkling. (Figure 42a and Figure 42b) The blank holders would keep tension on the work piece. Two kinds of blank holders are tested, a rigid blank holder (RBH) and a flexible blank holder (FBH). With the latter being able to adapt to the created geometry of the extended surface and therefore leads to less strain in the material than the same process with a rigid blank holder. Next to this the flexible blank holder needs least material in the blank holder, so has less waste material. After the forming process this extension still needs to be cut off. (Figure 42c) This cannot be done with a regular laser or plasma cutter, since it has become a three dimensional shape rather than a flat sheet. If holes and patterns are desired in the final product, these should be cut out after the forming as well. According to Ghang & Seonwoo (2012) the work piece could be torn during forming if it would already consist holes and patterns since this leads to unequal properties over the material surface.

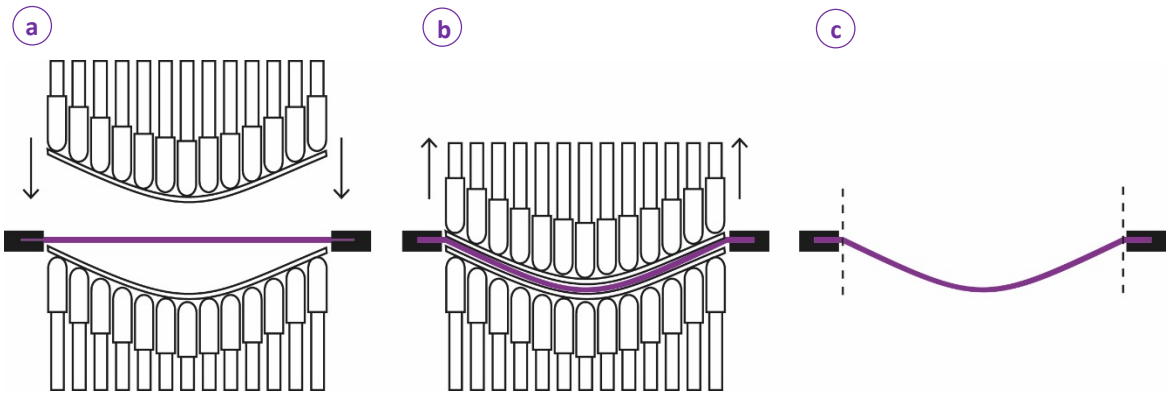

Figure 42: Visualisation of multipoint die forming with the use of blank holders to keep the workpiece stretched.

Incremental Sheet Forming

Another method to bend sheet metal is incremental sheet forming. Many variations on this method exist, such as Single Point Incremental Forming (SPIF), Two Point Incremental Forming (TPIF) and Double-Sided Incremental Forming (DSIF) which are visualized in Figure 43. (Zuo et al., 2017) In the Incremental Sheet Forming (ISF) process the work piece is clamped around its periphery and gradually deformed to the desired three dimensional shape by two strategically aligned pen-shaped tools that follow a pre-described path. (McCormick School of Engineering and Applied Science, Northwestern University, n.d.) These tools are positioned at opposite sides of the work piece and therefore can create concave as well as convex shapes and sharp elements. Compared to conventional sheet forming processes, ISF processes are highly versatile and flexible for the production of a small batch or customized parts. (Zuo et al., 2017) This makes it very suitable for architectural applications as well. A downside of this method is the fact that it is very time consuming compared to methods like (flexible) die stamping, since this method shapes the work piece by continuously sweeping the tools along a predefined path on the surface.

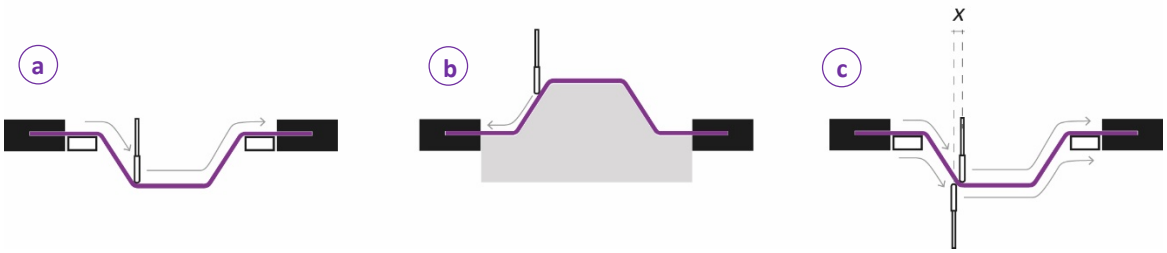

Figure 43: Three types of incremental sheet forming: Single Point Incremental Forming (SPIF) (a), Two Point Incremental Forming (TPIF) (b) and Double-Sided Incremental Forming (DSIF) (c).

Roll Forming

As discussed in Ghang & Seonwoo (2012) roller bending is the most general production method to create single-curved panels, but this method cannot create curvatures with very small radii. If a radius smaller than 200-300mm is desired one should use press forming. (Figure 44) However, these methods are not suitable for the production of double-curved panels.

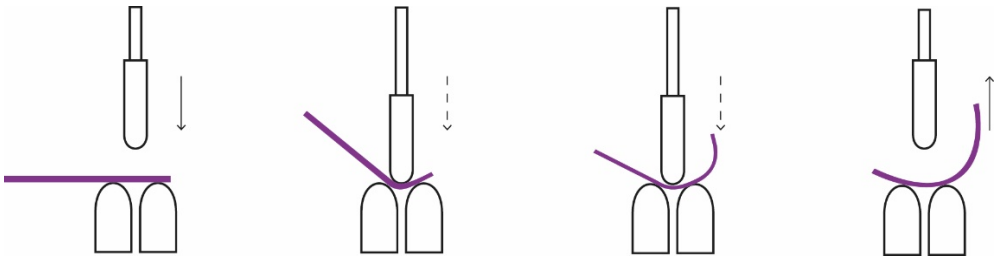

Figure 44: Principle of press forming, similar to roll forming (then a roll is used to continuously press the surface.

Springback of the final product

Springback is a phenomenon that occurs in metal forming after the forces used for bending are released, due to the elastic recovery of the metal. (Lal et al., 2017) This is a major problem in sheet forming, especially using high strength steel. Springback highly affects the accuracy of the final product. An addition to the above described Multipoint Forming methods which reduces the springback effect is the use of closed loop forming. (Li et al., 2014) The work piece is formed layer by layer and each layer the springback quantity is measured and compensated for in the next iteration. (Figure 45) This springback quantity is the difference between the actual shape and objective shape of each iteration. In this way the springback is reduced to reach a higher accuracy of the work piece.

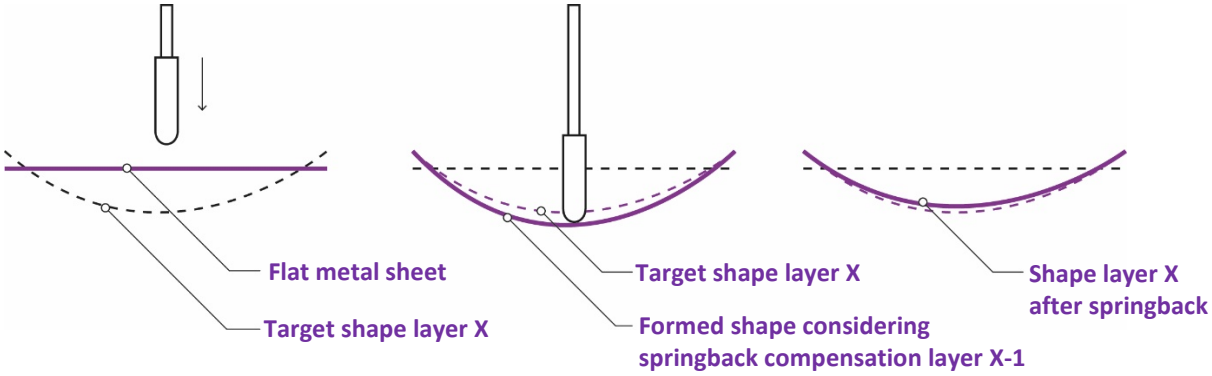

Figure 45: Principle of closed loop forming.

In Zuo et al. (2017) the authors propose a forming method based on Multipoint forming, but with a but with rotating parts on top of the pins that have an electromagnetic head. The magnetic heads are used to keep the work piece in place.

Distortion, tearing and wrinkling

As discussed before the work piece might tear or wrinkle during certain production methods. The tearing is mainly related to tensile instability and wrinkling to compressive instability. These distortions are mostly occurring in (highly) double-curved panels, due to the non-uniform distribution of forces. (Li et al., 2014) These differences in stresses lead to differences in strain and therefore distortions might occur. These distortions are very hard to control but can be avoided when using single-curved (developable) panels since the strain distribution is equally divided along the folding.

Increasing the stiffness of sheet metal

As described in the introduction, (double-)curved steel sheet can have many applications. Interior finishing, exterior finishing (facades), but also for self-supporting structures like pavilions. In a meeting with Mick de Haan from AIP Partners about the realisation of (double-)curved steel structures, in particular the MGM Park pavilions in Las Vegas, he explained these self-supporting pavilions were assembled from very thick curved steel plates up to a thickness of 25mm. (M. de Haan, personal communication, 24 October 2018) AIP Partners is a spin-off company from Royal IHC and still uses the factory and machining of the Royal IHC. They make use of heavy machines for the bending of plate metal, which are also used for the ship hulls they produce. However, these machines depend very much on the manual labour and experience of skilled workers and therefore it is time-consuming and difficult for curved plates, especially for double-curved plates, to reach the same accuracy as completely CNC controlled machines.

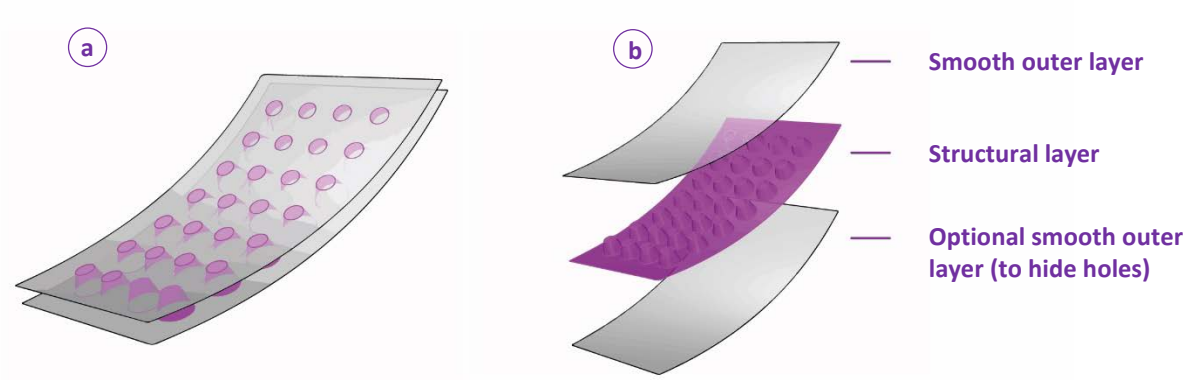

Figure 46: Visualization of sandwich structure proposed by Bailly et al. (2015).

Bailly et al. (2015) propose a different approach for the realization of self-supporting free-form metal structures. In principle they propose a metal sandwich structure which consists out of an inner and outer sheet welded on an inner framework, in order to use the loadbearing potential of the metal sheets. (Figure 46) By doing this the geometrical stiffness of the construction is increased, without adding more material. The inner framework, also known as the structural layer that holds the two panels together, consist out of conical shapes that can be arranged in a flexible way according to the stress distribution in the structure, with a minimal of 4 cones per panel that function as distance holders. For the purpose of their research the prototype is created using Stretch Forming (Figure 47a and Figure 47b) and Incremental Sheet Forming (ISF) (Figure 47c) using a CNC milled MDF die. This might not be the most waste-efficient way, but the panels are sorted in a way that the same MDF block can be re-milled and re-used. The authors also used aluminium sheets for the prototype, but they claim that the same method can be used for mild steel and even stainless steel grades. (Bailly et al., 2015)

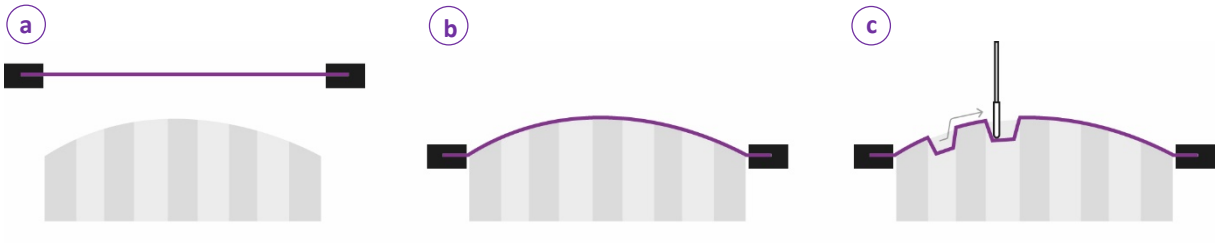

Figure 47: Used production method for creating sandwich panels, a combination between Stretch Forming and Incremental Sheet Forming.

D: Manual reconstruction of panel surfaces

Previously to the global approach, this approach will construct developable surfaces for the panels manually. As mentioned in section 7.2, this approach does not take into account adjacent panels so might lead to less smooth results. For the development and validation of this Grasshopper definition a cut-out of the case-study shape is used in order to have a topologically simple surface, which can be divided by a simple (u,v)-parameterization.

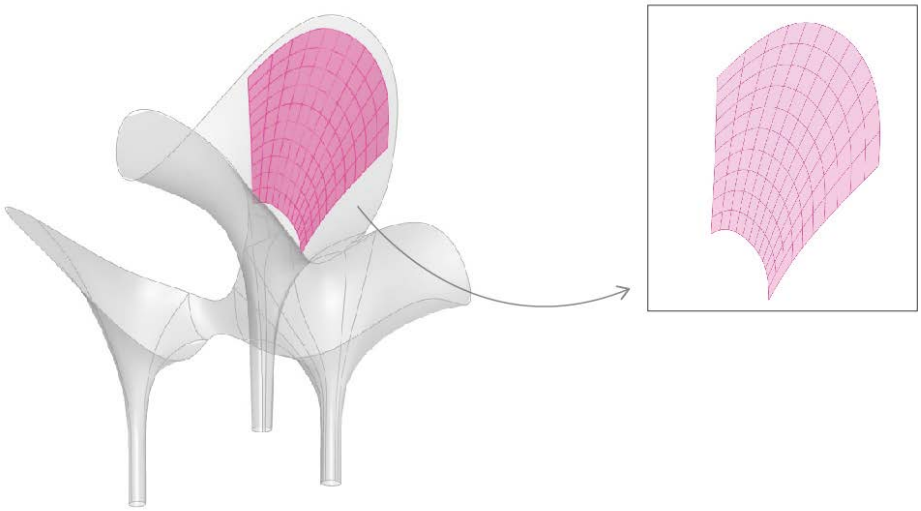

Figure 48: Cut out of double-curved shape as test surface for the Grasshopper definition of approach 2.

Setting up the definition

Lofting based on opposite spline curves

The most straight forward way to construct a developable surface based on 4 edge curves of a panel, is to select two opposite edge curves and loft them. In this way the original SSSS-surface is converted to a SRSR-surface. These abbreviations refer to the labelling of Tang et al. (2016), as described in Section 6.1.2. The original SSSS-surface consisted out of four spline curves which resembled the boundaries of a double-curved surface, whereas the created SRSR-surface consists out of two opposite spline curves and two opposite rulings in the order of Spline-Ruling-Spline-Ruling. The latter resembles the boundaries of a developable surface.

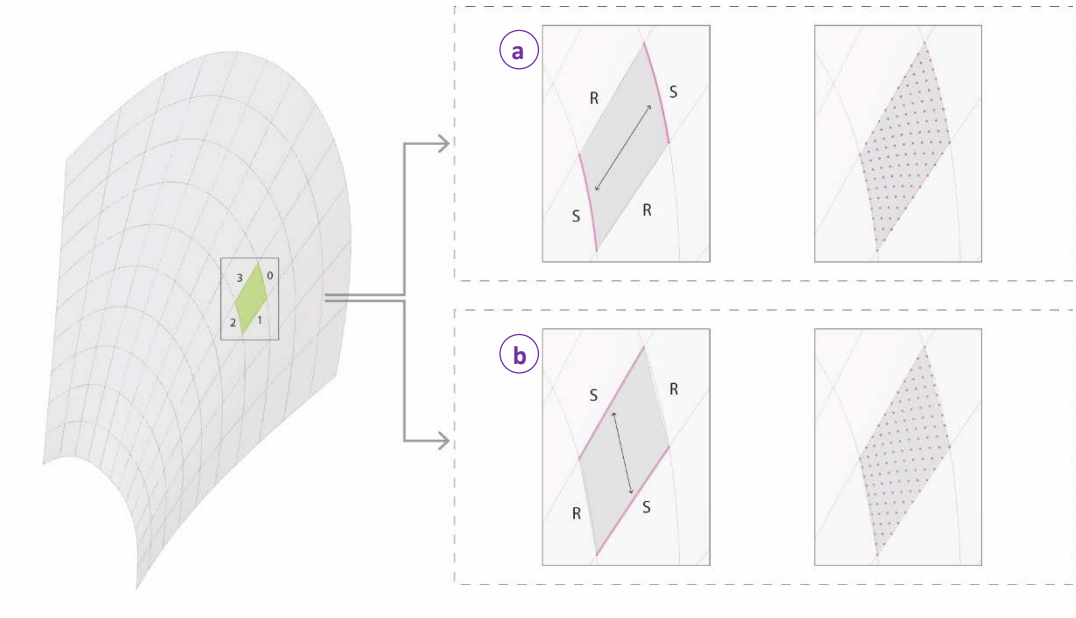

Figure 49: Close up of a panel reconstructed based on the lofting opposite curves. First based on the curves with index 0 and 2 (a), then based on the curves with index 1 and 3 (b). Both created surfaces are sampled at points densily distributed over the surface.

However, which set of opposite spline curves is selected for the lofting influences the accuracy of the end result. The definition creates the panels of both options as shown in Figure 49. Each panel is recreated as SRSR-surface (Figure 49a) and RSRS-surface (Figure 49b). Each created surface is sampled at a bunch of points of which the distance to the original SSSS-surface of the corresponding panel is measured. Which of the two created surfaces has the smallest average distance to the original panel surface, i.e. the one with the highest accuracy, will be chosen and replaces the corresponding SSSS-surface as shown in Figure 50.

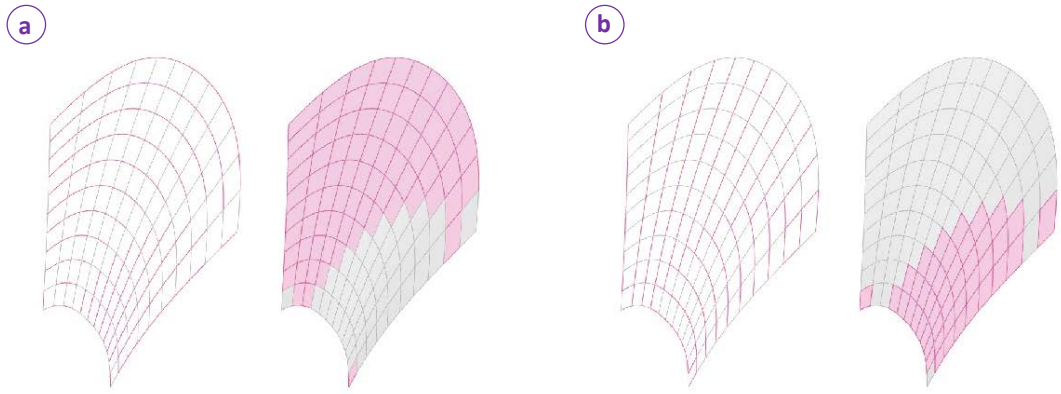

Figure 50: Created SRSR-surfaces for each panel (a) vs. created RSRS-surfaces for each panel (b). The highlighted panels are the panels that are chosen based on highest accuracy.

As a comparison, the different methods of surface recreation with their corresponding accuracies are listed in Table 7. The average panel dimensions in this example surface are 785x700 mm, this means that these deviations from the original surface are relatively small compared to the panel dimensions. Choosing the most accurate fit of the two different lofting directions leads to considerable improvements of the accuracy. However, it should be noted that the surface used in the development of this definition does not have extreme curvatures.

Table 8: Accuracy for each method of surface recreation based on the shape in Figure 50.

Method of recreating surface	Average distance to original surface	Average relative distance
SRSR-surfaces	1.39 mm	*0.19 %*
RSRS-surfaces	2.29 mm	*0.31 %*
Closest fit of the two above	0.32 mm	***0.04 %***

Based on the results thus far, this method seems to be simple and efficient. If this method is applied based on the complex shape with the quadrangular grid initialized in Section 7.2.1.2, the results are slightly different and the limitations of this method become visible. In Figure 51 can be seen for which panel the SRSR-surface (a) and for which panel the RSRS-surface (b) are chosen. In contrary with the simpler result shown previously, the direction of the lofts between the SRSR-surfaces themselves vary as well. This has to do with the fact that not only the shape is more complex, but more importantly the topology of the mesh with the singular vertices obstruct the panels from having similar orientations in simple (u,v)-parameter directions. These simply do not exist in this grid. However, the panels from Figure 51a will still be referred to as SRSR-surfaces and the panels from Figure 51b as RSRS-surfaces for the sole purpose to identify each panel based on the listed order of spline curves and rulings.

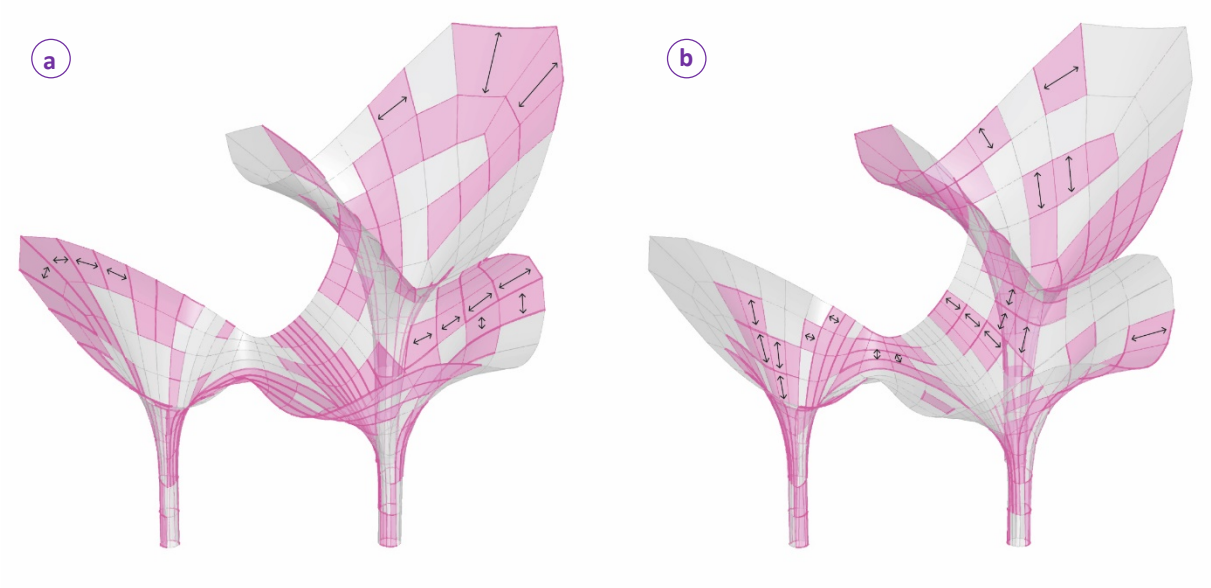

Figure 51: Created SRSR-surfaces for each panel (a) vs. created RSRS-surfaces for each panel (b). The highlighted panels are the panels that are chosen based on highest accuracy. The arrows in the image show the direction in which different lofts are created.

Table 8 shows the accuracy for both lofting directions as well as the accuracy for a combined solution where for each panel the lofting direction that is closest to the original shape is chosen. Since the panel dimensions differ significantly for each panel, the average relative distance is calculated slightly different. For each panel the average distance – based on the sample points – is divided by the average span of the panel (i.e. average edge length of the panel) in order to get the relative distance per panel. Then the average of all the independent relative distances is taken as the average relative distance. The results are less accurate than the results from the previous shape, possibly because of the higher curvatures.

Table 9: Accuracy for each method of surface recreation based on the shape in Figure 51.

Method of recreating surface	Average distance to original surface	Average relative distance
SRSR-surfaces	11.60 mm	*1.14 %*
RSRS-surfaces	11.94 mm	*1.16 %*
Closest fit of the two above	6.12 mm	***0.58 %***

More importantly, the limitations of this method become visible. At edges where panels that span different directions meet, there is a misalignment because one of the two edges is converted from a spline curve to a ruling. This phenomenon is shown in Figure 52. For smaller curvatures these misalignments are very minimal.

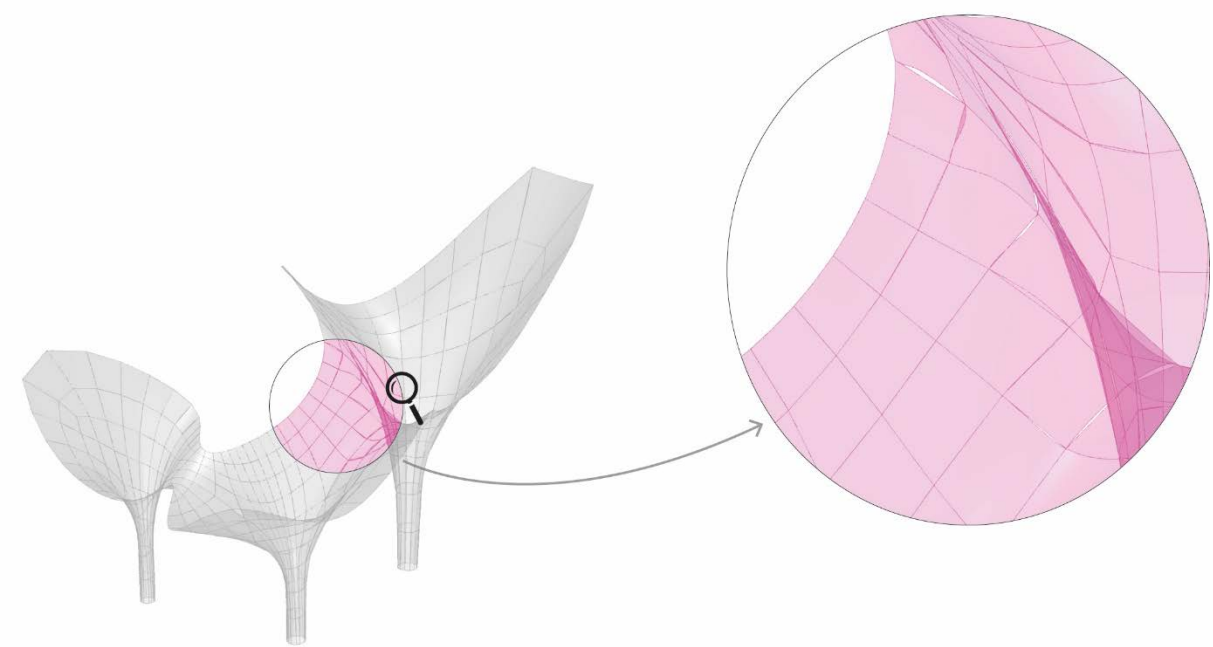

Figure 52: Misalignment of edges because one of the two edges is converted from a spline curve to a ruling.

Lofting based on the maximum principal curvature direction

Another way of recreating the panel surfaces is by manually creating a loft in the direction of the maximum principal curvature direction. This method comes closer to the method followed by Approach 1 (Section 7.2.3.1). In that method all normal vectors of the surface at the sample points are forced to lie parallel to the target plane, this target plane is initialized in the direction of the maximum principal curvature, so that the curvature lines in the minimum principal curvature direction are straightened (i.e. converted to rulings). In theory this method should provide a higher accuracy than the method where lofts are created from the opposite edge curves of the panels, so that the misalignments along the edges are minimized.

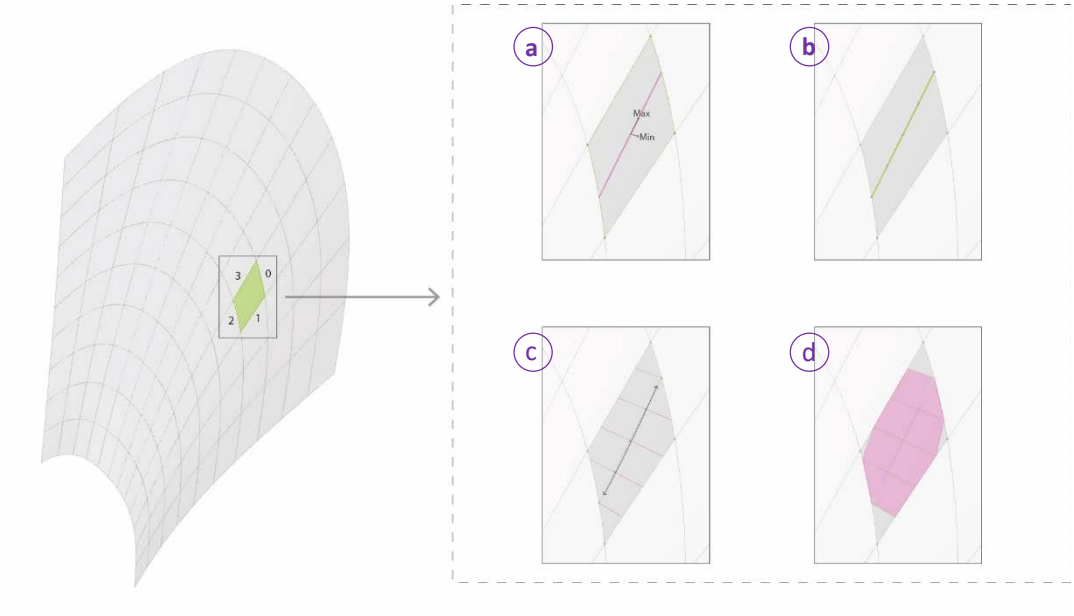

Figure 53: Rebuilding of the surface based on a loft in the direction of the maximum principal curvature of the panel at its centroid.

Figure 53 shows the different steps to create a loft as described above. At the centroid of each panel the surface is evaluated and the principal curvature directions at these points are retrieved. In the direction of the maximum principal curvature a geodesic curve is plotted on the surface. (Figure 53a) This curve is divided in a number of points (Figure 53b) and at each point a ruling is created perpendicular to this geodesic curve, i.e. in the direction of the minimum principal curvature. (Figure 53c) The created rulings form the basis for the loft as shown in Figure 53d.

However, the construction of a loft through the created rulings, should be extended to the boundaries of the panel. Unfortunately this is not yet developed and implemented in the Grasshopper definition since the global approach as discussed in section 7.2 is pursued because of the possibility for smoother results.